Journal of Applied Physics

Harmonic generation at the nanoscale

Cite as: J. Appl. Phys. **127**, 230901 (2020); https://doi.org/10.1063/5.0006093
Submitted: 27 February 2020 . Accepted: 25 May 2020 . Published Online: 15 June 2020

Luigi Bonacina, Pierre-François Brevet, Marco Finazzi, and Michele Celebrano

Journal of Applied Physics PERSPECTIVE scitation.org/journal/jap

Harmonic generation at the nanoscale

Cite as: J. Appl. Phys. **127**, 230901 (2020); doi: 10.1063/5.0006093
Submitted: 27 February 2020 · Accepted: 25 May 2020 ·
Published Online: 15 June 2020

View Online Export Citation CrossMark

Luigi Bonacina,[1] Pierre-François Brevet,[2] Marco Finazzi,[3] and Michele Celebrano[3,a)]

AFFILIATIONS

[1]Department of Applied Physics-GAP, Université de Genève, 22 Chemin de Pinchat, 1211 Geneva, Switzerland
[2]Institut Lumière Matière, UMR CNRS 5306, Université Claude Bernard Lyon 1, 10 Rue Ada Byron, F-69622 Villeurbanne Cedex, France
[3]Dipartimento di Fisica, Politecnico di Milano, Piazza Leonardo da Vinci 32, 20133 Milano, Italy

[a)]**Author to whom correspondence should be addressed:** michele.celebrano@polimi.it

ABSTRACT

Nonlinear photon conversion is a fundamental physical process that lies on the basis of many modern disciplines, from bioimaging and theranostics in nanomedicine to material characterization in materials science and nanotechnology. It also holds great promise in laser physics with applications in information technology for optical signal processing and in the development of novel coherent light sources. The capability to efficiently generate harmonics at the nanoscale will have an enormous impact on all these fields, since it would allow one to realize much more compact devices and to interrogate matter in extremely confined volumes. Here, we present a perspective on the most recent advances in the generation of nonlinear optical processes at the nanoscale and their applications, proposing a palette of future perspectives that range from material characterization and the development of novel compact platforms for efficient photon conversion to bioimaging and sensing.

I. INTRODUCTION

Although multiphoton processes had already been predicted in the 1930s (Göppert-Mayer, 1931), experimentalists had to wait for the introduction of the laser (Maiman, 1960) before they could provide the first proof of harmonic generation (Franken *et al.*, 1961), an observation that marked the outbreak of nonlinear optics. In a perturbative approach, nonlinear optical phenomena are classified according to the number of photons simultaneously involved (Boyd, 1984). Lower order nonlinear phenomena—involving only three or four photons—are most widely investigated and exploited for non-invasive optical studies of matter, owing to their detectable yields granted by the large values of the corresponding second- and third-order nonlinear susceptibilities, $\overleftrightarrow{\chi}^{(2)}$ and $\overleftrightarrow{\chi}^{(3)}$. Second harmonic generation (SHG) is a $\overleftrightarrow{\chi}^{(2)}$-related process, whereby two impinging photons of the same energy, interacting with matter, generate a third photon at twice the energy in a coherent fashion [Fig. 1(a)]. If the energy degeneracy is lifted, the energy of the generated photon may be either the algebraical sum or the algebraical difference of the impinging photon energies. These phenomena are known as sum and difference frequency generation (SFG and DFG), respectively [Figs. 1(b) and 1(c)]. Similarly, the excitation of matter with a single impinging photon can trigger the emission of two output photons with a total energy equal to one of the exciting photons [Fig. 1(d)]. This process is known as spontaneous parametric downconversion (SPDC). Instead, third-order nonlinear processes involve the interaction of four photons. Therefore, one can attain a variety of mixing processes, commonly known as Four Wave Mixing (FWM). Examples of such processes are (i) two impinging photons producing two photons at different energies and (ii) three impinging photons generating a single outgoing photon [Figs. 1(f) and 1(g)]. The FWM process, where three incoming photons having the same energy, generates a fourth 3-fold more energetic photon, is also known as Third Harmonic Generation (THG) [Fig. 1(e)], the third-order equivalent of SHG. The above described processes are also defined as parametric, since the initial and final quantum-mechanical states of the system interacting with light are the same.

The integration of optical processes at the nanoscale may become fundamental in fields such as quantum optics as well as in biology and medicine. The ability to generate nonlinear optical processes in nanoscale volumes may allow boosting the efficiencies of high throughput screening techniques and squeezing optical logic functions down to electronic chip scales, pointing toward the realization of nonlinear optical sensing probes and photonic sources operating at the nanoscale. The spatial confinement of light below

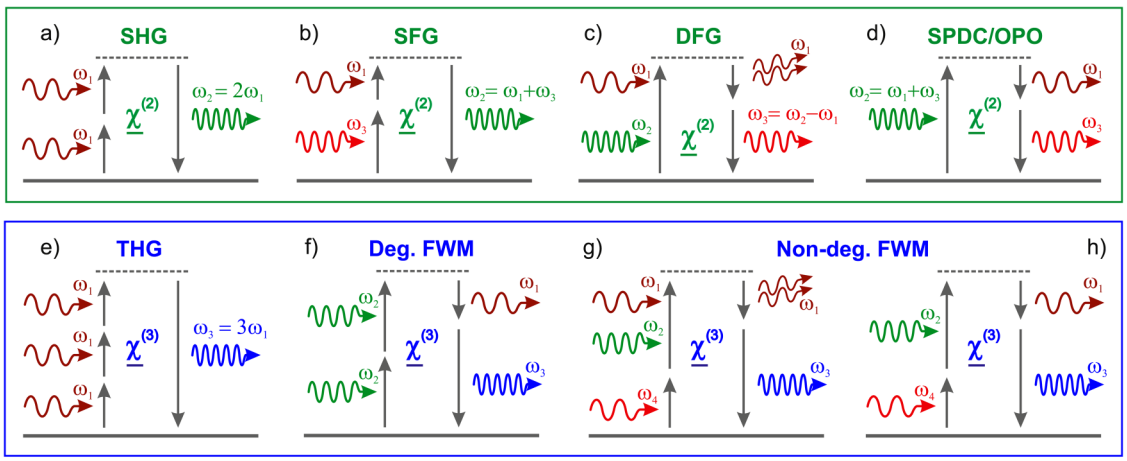

FIG. 1. Energy level schemes of second (top) and third order (bottom) nonlinear optical processes. (a)–(d) Three photon wave mixing processes mediated by the second-order nonlinear susceptibility $\overleftrightarrow{\chi}^{(2)}$. The nonlinear conversion between photons with energy degeneracy produces (a) second harmonic generation (SHG), while non-degenerate photons undergo (b) sum frequency generation (SFG), (c) difference frequency generation (DFG) as well as (d) spontaneous parametric downconversion (SPDC) or optical parametric oscillation (OPO). (e)–(h) Four photon wave mixing processes mediated by the third-order nonlinear susceptibility $\overleftrightarrow{\chi}^{(3)}$. The nonlinear combination involving three or two degenerate photons give origin to (e) third harmonic generation (THG) or degenerate four wave mixing (FWM), while coherent combinations of three non-degenerate photons produce [(g) and (h)] non-degenerate FWM. (c) and (g) represent stimulated processes, while (d) and (h) are the corresponding spontaneous ones.

the operational wavelength is nowadays a standard procedure, which is attained, for example, by exploiting localized or propagating surface plasmons (Schuller *et al.*, 2010). On the other hand, obtaining efficient light conversion at the nanoscale through nonlinear optical processes remains an open challenge, since the common mechanisms—e.g., phase-matching—adopted in bulk and integrated optics (Dimitropoulos *et al.*, 2004) cannot be applied in volumes confined below the wavelength of light.

This perspective presents future possibilities disclosed by the developments and applications of parametric multi-photon processes in nanostructured matter and nanoscale systems. These phenomena are typically described within a perturbative quantum mechanical approach to light–matter interaction (Boyd, 1984). Nevertheless, quasi-classical models are often sufficient to account for them. In this context, light–matter interaction is embedded in the nonlinear susceptibilities, $\overleftrightarrow{\chi}^{(n)}$, which describe the nonlinear relation between the local electric field and the material polarizability. These tensors must be invariant with respect to the same symmetry group of the material they describe, a rule known as the Neumann principle (Nye, 1957). An important spatial transformation is the invariance through inversion by a central point, known as central symmetry. Third-order nonlinear processes are allowed in media possessing a center of inversion like gases, liquids, or centrosymmetric crystalline solids, which constitute the majority of natural materials. Conversely, parametric second-order processes such as SHG are forbidden in centrosymmetric materials by the electric dipole emission selection rules (Kleinman, 1962). This explains why efficient frequency doubling can only be achieved in non-centrosymmetric crystals (Chemla and Zyss, 1987). Nevertheless, second harmonic scattering (SHS), or incoherent SHG, also known as hyper Rayleigh scattering (HRS), can be observed in some centrosymmetric materials albeit with a much weaker intensity when instantaneous orientational fluctuations break this rule (Terhune *et al.*, 1965 and Clays and Persons, 1991). Similarly, coherent SHG has also been observed in centrosymmetric materials when the electric dipole approximation restriction is relaxed (Duboisset and Brevet, 2018) or at the interface between centrosymmetric media (Shen, 1989 and Eisenthal, 1992). In the electric dipole approximation, the spatial phase of the electromagnetic fields is neglected and therefore coherent SHG cancels in all media invariant under the inversion symmetry also known as centrosymmetry. Hence, at the interface between centrosymmetric media, inversion symmetry breaks down.

Soon after the seminal nonlinear optical experiment reporting the SHG response from a quartz crystal in 1961 (Franken *et al.*, 1961), the identification of efficient nonlinear materials required the availability of single crystals with a reasonably large size combined with good optical and dielectric quality. This problem was alleviated in 1968, when Kurtz and Perry proposed the powder technique (Kurtz and Perry, 1968). The observation of multiphoton parametric processes in single nanoscale systems was observed much later, after advanced laser sources combined with enhanced detection instrumentation became available (Bouhelier *et al.*, 2003). SHG has been observed from individual non-centrosymmetric dielectric nanoparticles (Bonacina *et al.*, 2007; Nakayama *et al.*, 2007; and Hsieh *et al.*, 2009), from plasmonic nanoparticles, unsupported (Butet *et al.*, 2010a; 2010b) and supported on a substrate (Zavelani-Rossi *et al.*, 2008) as well as from unsupported plasmonic-dielectric hybrid nanostructures (Pu *et al.*, 2010). More recently, higher order frequency conversion like third- and fourth-harmonic generation and FWM have also been demonstrated (Lippitz *et al.*, 2005; Kachynski *et al.*, 2008; Rogov *et al.*, 2015b; Liu *et al.*, 2018; and Riporto *et al.*, 2019).

In this perspective, we will address the most recent advances in harmonic generation at the nanoscale and the most promising applications deriving from the engineering and enhancement of nonlinear optical effects in extremely confined volumes. Section II presents a survey of the physical mechanisms at play in harmonic generation at the nanoscale, while Sec. III shows how the generation of harmonics can be employed as a local probe to investigate the nanoscale properties of matter. Section IV focuses on the most recent efforts in engineering light–matter interaction at the nanoscale to artificially enhance the harmonic generation and on the perspective of engineering metasurfaces to obtain new ultra-flat nonlinear materials. Section V gives an overview on the application of harmonic-generating nanostructures as effective probes for bio-oriented applications (i.e., optical sensing and bio-imaging). Finally, Sec. VI presents a perspective concerning the employment of parametric amplification to enhance the harmonic generation in extremely confined volumes by means of an external seed beam to foster its application in bio-oriented experiments.

II. HARMONIC GENERATION AT THE NANOSCALE

In nanoscale systems, the phase matching condition for the efficient generation of harmonics cannot be met since the size of the nano-object, L, is typically much smaller than the excitation field wavelength λ. One can instead exploit the local field enhancement of the incident fundamental and emerging harmonic intensities. In particular, resonances in nanoscale structures, for instance, localized surface plasmon or Mie resonances, lead to electromagnetic field localization and amplitude enhancements. Therefore, at the nanoscale, symmetry also becomes a critical criterion to identify non-zero macroscopic susceptibility tensors to enhance even-order nonlinear processes such as SHG. For instance, because of their central symmetry, liquids do not often sustain sizeable SHG as in common second-order nonlinear media. Let alone symmetry, the magnitude of the elements of the third-rank $\overleftrightarrow{\chi}^{(2)}$ tensor depends on the nature of the material, be it organic, inorganic, or metallic. Efficient materials for frequency doubling are usually of dielectric nature with large bandgaps to avoid re-absorption of the SHG wave. The most common materials employed for SHG are potassium dihydrogen phosphate (KDP) or trihydrogen phosphate (KTP) (Eckardt *et al.*, 1990) because of their relatively large bandgap (350 nm–4500 nm) and phase-matching range (984 nm–3400 nm) covering the whole visible range up to the near infrared (Yariv, 1995). KTP is also among the first materials that has been synthesized into nanoparticles for bioimaging (Le *et al.*, 2008 and Mayer *et al.*, 2013). In fact, ensemble measurements of SHG efficiency performed by HRS on colloidal suspensions of non-centrosymmetric nanocrystals generally provide values consistent with the bulk ones (at least for larger particles) (Joulaud *et al.*, 2013). Therefore, materials known for their good nonlinear properties and with a broad transparency range in the spectral region selected for excitation and emission are often the first choice for applications. More recently, lithium niobate ($LiNbO_3$) (Niederberger *et al.*, 2004; Timpu *et al.*, 2019a; and Riporto *et al.*, 2019) or barium titanate ($BaTiO_3$) (Hsieh *et al.*, 2010; Culic-Viskota *et al.*, 2012; Kim *et al.*, 2013; and Sun *et al.*, 2019) have been proposed for their superior nonlinear susceptibility, but the quest for more and more efficient materials still goes on. For example, $BiFeO_3$ has also recently been identified for its efficiency toward SHG (Schwung *et al.*, 2014). Two-dimensional dichalcogenides (Hsu *et al.*, 2014) as well as plasmonic materials (Naik *et al.*, 2013)) have been proposed as efficient materials for SHG. Binary III-V or II-VI semi-conducting materials and perovskites also provide interesting routes, although the presence of heavy metals in the latter case might pose environmental and health issues (Kasel *et al.*, 2019).

Although in bulk centrosymmetric media, such as metals, $\overleftrightarrow{\chi}^{(2)}$ is expected to vanish, the presence of interfaces and nanoscale defects is often associated with sizeable second-order nonlinear effects. Indeed, surfaces, interfaces, as well as local defects are spatial regions where the central symmetry is removed (Bloembergen and Shen, 1966; Chen *et al.*, 1981; and Sipe *et al.*, 1980). Low-dimensional systems, moreover, may sustain strong electromagnetic field gradients, which introduce strong contributions from higher order multipoles, breaking inversion symmetry and thus allowing for the recovery of non-zero susceptibilities and, hence, of sizeable SHG responses. While this concept was first proposed for extended systems, it holds important implications and effects in nanoscale systems, where the ratio between surface area and bulk volume dramatically increases. Consequently, despite the bulk material central symmetry and strong absorption in the UV–visible–IR region of the electromagnetic spectrum, metallic (e.g., gold and silver) nanostructures have been proposed for enhancing second-order nonlinear processes at the nanoscale. Unexpectedly, high SHG yields and large second-order susceptibilities have been recently reported (Zhang *et al.*, 2011 and Celebrano *et al.*, 2015), thanks to the large resonant enhancement of the electromagnetic fields provided by localized surface plasmon resonances (LSPRs), which compensate for the abovementioned disadvantages. In nanostructures, the resonant enhancement of SHG can be achieved both at the fundamental and the harmonic frequency. This possibility arises from the dramatic dependence of the LSPR wavelength on the material, size, shape, and environment of the nanostructures. This line of research, which will be described in detail in Sec. IV A, is still receiving considerable attention and will likely be pursued further as the possibility of realizing finely designed nanostructures is enabled by the recent improvements of standard nanofabrication methods, such as focused ion beam (FIB) and e-beam lithography (EBL). In particular, the resolution of FIB is recently benefiting from the employment of helium ions for the milling beam, which allows fabricating features below the nanometer (Boden *et al.*, 2011). Such a resolution is, at the moment, out of reach of EBL, which is however less expensive and time consuming for the realization of extended structures.

Yet, matching the fundamental and harmonic frequencies with LSPR frequencies is not the only criterion to design efficient nanostructures. It is also important to achieve mode matching, namely, the best overlap of the charge distributions of the fundamental and harmonic modes associated with the corresponding LSPRs. Mode matching in plasmonic nanostructures replaces the older concept of Miller's rule operating at the macroscopic scale for many different materials (Celebrano *et al.*, 2015; O'Brien *et al.*, 2015; and Butet *et al.*, 2016). Miller's rule states that the nonlinear susceptibility tensor $\overleftrightarrow{\chi}^{(2)}$ scales with the ratio of the linear

susceptibility tensors $\overleftrightarrow{\chi}^{(1)}$ at the fundamental and harmonic frequencies. Mode matching in plasmonic nanostructures can only be obtained with a careful design of the nanostructures and further improvement can be obtained along this line with more advanced structures, possibly with the aid of computer-assisted methods (Malkiel *et al.*, 2018). In this frame, the exploitation of Fano profiles has, for instance, been proposed, where the combination of a broadband and a narrow resonance may lead to favorable sharp peak-valley spectral features (Bachelier *et al.*, 2008). Besides mode matching, polarization matching must also be fulfilled before any resonance enhancement can occur. The role played by this rule has been clearly underlined in a study of the SHG resonance from supported gold nanorods (Hubert *et al.*, 2007).

III. HARMONIC GENERATION AS A PROBE FOR NANOSCALE PROPERTIES

The nanoparticle size is intimately hooked to the mode description of the SHG response, which therefore may become a fundamental tool for characterizing nanoscale colloids. In particular, as size grows, the electric dipole approximation is no longer valid and higher order electromagnetic modes appear with specific charge distributions and therefore specific angular and polarization patterns in the far field for the SHG response. Therefore, switching from one mode to another may lead to dramatic changes in the SHG intensity and in its angular or polarization distribution. A specific example may be illustrated with SHS from spherical gold nanoparticles dispersed as a liquid suspension. For the same couple of fundamental and harmonic frequencies, for instance, for 800 nm and 400 nm, respectively, the dipolar mode will dominate for small sizes of about 20 nm with the strongest SHS intensity collected for both the fundamental and harmonic light polarized perpendicular to the plane of scattering, whereas, for sizes larger than about 100 nm, the strongest SHS intensity will be obtained for second harmonic light polarized perpendicular to the plane of scattering but for fundamental light polarized at $\pi/4$ with respect to the plane of scattering (Nappa *et al.*, 2005 and Russier-Antoine *et al.*, 2007).

Since SHG in metallic nanoparticles is due to the surface, the shape of the nanostructures plays a crucial role. For unsupported nanostructures, like liquid suspensions of nanoparticles, this feature is essential in predicting the properties of SHG light. Nanostructures with a centrosymmetric shape like spheres, rods, or cubes will therefore exhibit a strongly retarded response due to the cancellation of the local electric dipole contribution to the SHG response. Retardation is the property accounting for the time delay between all contributions to the total SHG response. It is often described through a multipolar expansion where the electric dipole constitutes the first order dominating the next orders and, in particular, the electric quadrupole one. For nanoparticles with a centrosymmetric shape, the electric dipole contribution vanishes, and the next orders of the multipolar expansion become clearly visible (see Fig. 2). It is however expected that, for non-centrosymmetric nanostructures like prisms, retardation would play a much less important role. Therefore, competition between symmetry and retardation translates into a competition between size and shape, leading to characteristic SHG light properties and corresponding angular and polarization patterns, as seen in Fig. 2 (Duboisset *et al.*, 2019). In perspective, this simple method may become a routine analytical method for the characterization of nanoparticle samples.

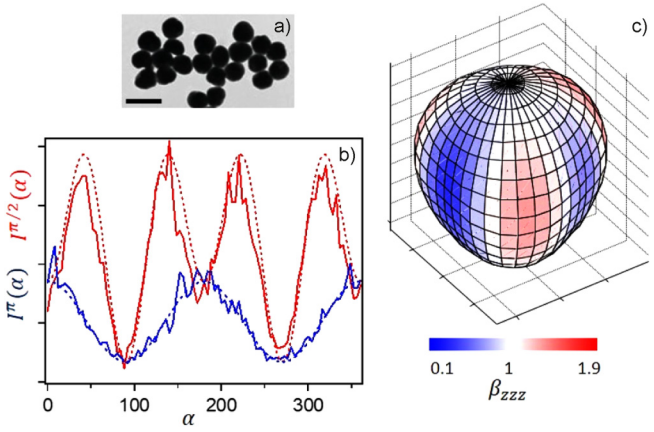

FIG. 2. SHG scattering shape determination of an aqueous suspension of 100 nm diameter gold nanoparticles. (a) Transmission Electron Microscopy (TEM) image, scale bar is 200 nm, (b) fundamental linearly polarized (angle α) dependence of the SHG scattered light in the right-angle $I^{\pi/2}(\alpha)$ and $I^{\pi}(\alpha)$ forward directions of collection, (solid line) experimental data, (dotted line) corresponding multipolar expansion adjusted fits, (c) reconstruction of the average 3D shape of the 100 nm diameter gold nanoparticles as seen by polarization resolved SHG scattering. Image reproduced with permission from Duboisset *et al.* J. Phys. Chem. C **123**, 25303–25308 (2019). Copyright 2019 American Chemical Society.

Recently, more advanced nanostructures have been proposed, thanks to the versatility of lithographic techniques. Arrays of such nanostructures, also termed metasurfaces (Krasnok *et al.*, 2018) (see Sec. IV B), have hence been designed with a great variety in their SHG response. Interestingly, the substrate, which breaks the initial symmetry of the structures, plays a fundamental role in determining the nonlinear optical properties of the structure and provides it with another degree of complexity that may be used for refined engineering. Likewise, with structures dispersed in a homogeneous matrix, complex geometries have been synthesized from multi-material core-shell to metallic urchins-like nanostructures. Among them, one promising avenue is the design of chiral nanostructures. Chiral nano-springs indeed exhibit SHG optical activity signals 10^5 times larger than those observed in the linear regime (Kolkowski *et al.*, 2015, Collins *et al.*, 2019, and Valev *et al.*, 2010).

The generation of harmonics can also be applied for the characterization of 2D materials, such as graphene and transition metal dichalcogenides (2DMDs), which are recently drawing more attention in the field of nanophotonics for their unique optical properties and intense interaction with light at the nanoscale (Bonaccorso *et al.*, 2010; Koppens *et al.*, 2011; and Manzeli *et al.*, 2017). In particular, the high degree of symmetry in single layer graphene (SLG) pushed researchers to investigate its potential implementation as an atomically flat THG source (Kumar *et al.*, 2013 and Hong *et al.*, 2013). Although it has been shown that third-order nonlinear properties of SLG are not superior than other existing materials (Khurgin, 2014), researchers recently demonstrated that it is

possible to dramatically increase its THG efficiency by electric doping (Soavi *et al.*, 2018). On the other hand, the lack of SHG in SLG can be exploited as a powerful tool, since appearance of SHG directly reveals its assembly in multilayers (Dean *et al.*, 2010). Despite the negligible SHG expected in SLG, it has been theoretically predicted that light confinement in graphene nanoflakes could significantly enhance SHG in these nanoscale systems (Yu *et al.*, 2016), making graphene nanoflakes potential candidates as compact platforms for nonlinear sensing. Notably, large values of nonlinear polarizability have been also very recently demonstrated in graphene oxide flakes through hyper Rayleigh scattering (HRS) experiments (Russier-Antoine *et al.*, 2020). This may lead to new applications of graphene-oxide based nanomaterials in second-order nonlinear optics. Conversely, in the majority of other 2DMD, the SHG efficiency can be rather large due to the lack of inversion symmetry and has been already employed to directly reveal the underlying symmetry and crystal orientation in these materials (Li *et al.*, 2013 and Malard *et al.*, 2013).

Thanks to the surface origin of their SHG response, nonlinear plasmonic nanostructures are expected to yield an extreme sensitivity to the local environment. Surfactant substitution or protein adsorption have been successfully performed with plain metallic nanoparticles, leading to the possibility of achieving a sensitivity as good as that obtained in the linear optical regime (El Harfouch *et al.*, 2014 and Russier-Antoine *et al.*, 2008). Preliminary works have nevertheless clearly identified other morphologies, like core–shell or sharply tipped systems, for best performances in sensing (Butet *et al.*, 2012; Butet *et al.*, 2013; and Mesch *et al.*, 2016). However, considering the extreme surface sensitivity of SHG in plasmonic systems, sensing platforms based on this nonlinear mechanism could be exceedingly sensitive to the molecular species binding to their surface and locally modifying the surface charges. Similarly, other platforms like 2DMD nanoscale flakes should receive further attention as their SHG response is highly dependent on their environment, including deformation induced by external strain (Mennel *et al.*, 2018 and Yamashita *et al.*, 2019). In the same direction, it has been shown that the quantum effects in individual single layer graphene of sizes confined to the nanoscale allow for efficient generation of harmonics (Yoshikawa *et al.*, 2017 and Cox *et al.*, 2017). In this framework, it is theoretically expected that also even-order harmonics, such as SHG, can be effectively attained in nanostructured graphene (Majérus *et al.*, 2017), therefore opening interesting perspectives in the application of nanostructured graphene as a potential platform for enhanced nonlinear sensing.

IV. ENGINEERING HARMONIC GENERATION AT THE NANOSCALE

A. Enhanced harmonic generation at the nanoscale

In the past decades, researchers dedicated intense efforts in devising nanostructures to further boost the weak nonlinear optical processes at the nanoscale. One of the most successful approaches to compensate for the lack of phase matching conditions in sub-wavelength regions (Kauranen *et al.*, 2012) is the exploitation of the intense field enhancements stemming from the plasmonic resonances in noble metal nanoantennas. Nanoantennas are nanostructured devices engineered to efficiently converting free propagating optical radiation into localized energy and vice versa (Novotny and Van Hulst, 2011 and Biagioni *et al.*, 2012). Third Harmonic Generation (THG) was the first to be reported in plasmonic nanoparticles (Lippitz *et al.*, 2005), because of the high degree of symmetry in metals. More recently, plasmonic gap nanoantennas demonstrated to be the ideal platforms to boost third order nonlinear optical effects, such as THG and FWM (Hanke *et al.*, 2009 and Harutyunyan *et al.*, 2012) [Figs. 3(a) and 3(b)], thanks to the large localized fields produced in the interstitial space between the two antenna elements (Novotny *et al.*, 2011 and Biagioni *et al.*, 2012). To circumvent the limits imposed by symmetry in metals and access the selection rules for second order nonlinear processes (Finazzi *et al.*, 2007), broken-symmetry nanostructures have been realized obtaining rather efficient dipolar emission of SHG (Kauranen and Zayats, 2012; Butet *et al.*, 2015; Celebrano *et al.*, 2015; Black *et al.*, 2015; and Gennaro *et al.*, 2016) [Figs. 3(h) and 3(i)]. Efficient plasmon-enhanced SHG can be attained since, due to the selection rules at play, the nonlinear dipole sources in metals that radiate in the far field are mainly associated with surfaces, i.e., at the interface with the dielectric environment. A specific care was dedicated to the development of multi- resonant nanoantennas, where the main plasmonic resonances would overlap with both the excitation as well as the emission wavelength (Thyagarajan *et al.*, 2012 and Celebrano *et al.*, 2015). This strategy, along with a broken-symmetry geometry, allows obtaining a $\chi^{(2)}_{eff}$ that is as high as 150 pm/V (Celebrano *et al.*, 2015), which is comparable with the most efficient nonlinear nanocrystals (Rogov *et al.*, 2015a). It is here worth stressing that the reported $\chi^{(2)}_{eff}$ in plasmonic nanostructures is a lower-bond value, since in these systems only the surface plays a role in SHG.

Given the remarkably high efficiency attained at the nanoscale, individual plasmonic nanoantennas were recently exploited also for ultrafast pulse characterization (Extermann *et al.*, 2008; Accanto *et al.*, 2014; and Gennaro *et al.*, 2018). In perspective, the possibility of finely tuning the geometry of plasmonic nanoantennas using modern lithographic techniques would allow one to further enhance nonlinear processes at the nanoscale through cascaded nonlinear processes (Celebrano *et al.*, 2019) and envision their employment also as nanoscale parametric amplifiers (Zhang *et al.*, 2016).

However, plasmonic materials (i.e., metals) display large losses at optical frequencies, which are associated with relatively low damage thresholds that can mitigate the benefits of the field enhancements in nanoantenna realizations. In this respect, intense efforts have been recently dedicated to devise nanoantennas based on dielectric materials, because of the extremely low losses at optical frequencies (Kuznetsov *et al.*, 2016) and rich variety of resonant multipoles, both magnetic and electric, that can be engineered. Despite the rather low Q factors characteristic of these modes, low losses along with the choice of high refractive index materials allow attaining efficient nonlinear processes at the nanoscale (Smirnova *et al.*, 2016). After the first demonstrations of efficient THG on nanodisks of centrosymmetric materials, such as Si (Shcherbakov *et al.*, 2014) and Ge (Grinblat *et al.*, 2016) [Figs. 3(c) and 3(d)], efficient SHG was soon after also induced in nanopillars composed of non-centrosymmetric semiconductors, such as AlGaAs (Gili *et al.*, 2016) and GaAs (Liu *et al.*, 2016) [Figs. 3(j) and 3(k)]. A further possibility to boost the harmonic generation in dielectric-

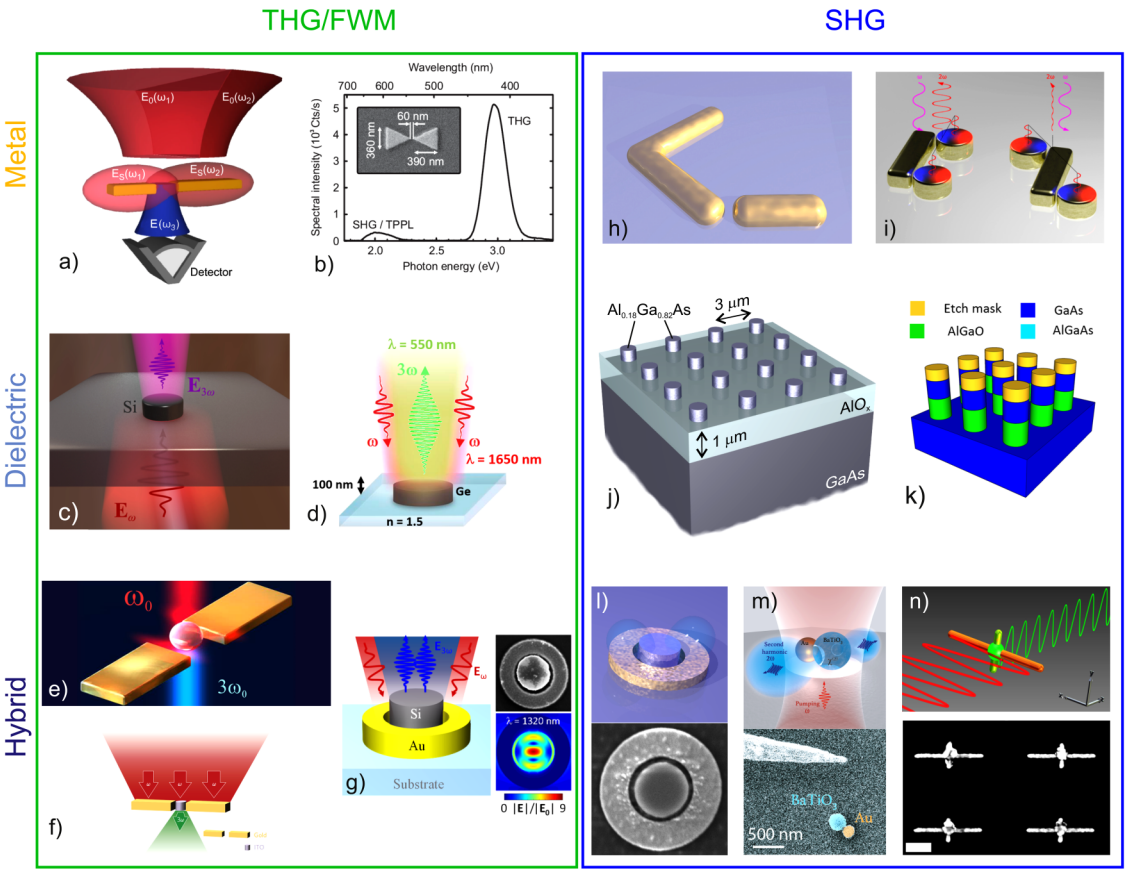

FIG. 3. Strategies to enhance harmonic generation at the nanoscale. (a)–(g) Nanoscale platforms to enhance THG and FWM. (a) Doubly resonant plasmonic gap nanoantenna (Harutyunyan *et al.*, 2012) and (b) bowtie plasmonic nanoantenna (Hanke *et al.*, 2009) devised to boost FWM and THG, respectively. (c) Silicon (Si) (Shcherbakov *et al.*, 2014) and (d) germanium (Ge) (Grinblat *et al.*, 2016) nanodisks with optimized radii to enhance THG. (e)–(f) Gap plasmonic nanoantennas coupled with nonlinear active nanocrystals to boost THG through optimized pump field localization (Metzger *et al.*, 2014 and Aouani *et al.*, 2014). (g) Si nanodisk hybridized with a plasmonic disk to enhance the THG emission from the bulk of silicon (Shibanuma *et al.*, 2017). (h)–(n) Nanoscale platforms to enhance SHG. Broken symmetry geometries in plasmonic nanoantennas to circumvent the selection rules for efficient SHG emission (h) (Celebrano *et al.*, 2015) or, in other words, optimize the near-field phase of SHG (i) (Gennaro *et al.*, 2016). Nanopillars of non-centrosymmetric dielectric material on transparent substrate (j) (Gili *et al.*, 2016 and Ghirardini *et al.*, 2017) or suspended (k) (Liu *et al.*, 2016) to optimize the field confinement at the pump and SH wavelengths. (l)–(n) Hybrid systems where the plasmonic nanostructure allows concentrating the pump field into the nonlinear dielectric nanostructure and improving the outcoupling of SHG (Gili *et al.*, 2018; Renaut *et al.*, 2019; and Linnenbank *et al.*, 2016). Panel (a) reproduced with permission from Harutyunyan *et al.*, Phys. Rev. Lett. **108**, 217403 (2012). Copyright 2012 American Physical Society. Panel (b) adapted from Hanke *et al.*, Phys. Rev. Lett. **103**, 257404 (2009). Creative Commons Attribution 3.0 License. Panel (c) reproduced with permission from Shcherbakov *et al.*, Nano Lett. **14**, 6488–6492 (2014). Copyright 2014 American Chemical Society. Panel (d) reproduced with permission from Grinblat *et al.*, Nano Lett. **16**, 4635–4640 (2016). Copyright 2016 American Chemical Society. Panel (e) reproduced with permission from Metzger *et al.*, Nano Lett. **14**, 2867–2872 (2014). Copyright 2014 American Chemical Society. Panel (f) reproduced with permission from Aouani *et al.*, Nat. Nanotechnol. **9**, 290–294 (2014). Copyright 2014 Springer Nature. Panel (g) reproduced with permission from Shibanuma *et al.*, Nano Lett. **17**, 2647–2651 (2017). Copyright 2017 American Chemical Society. Panel (h) reproduced with permission from Celebrano *et al.*, Nat. Nanotechnol. **10**, 412–417 (2015). Copyright 2015 Springer Nature. Panel (i) reproduced with permission from Gennaro *et al.*, Nano Lett. **16**, 5278–5285 (2016). Copyright 2016 American Chemical Society. Panel (j) reproduced with permission from Ghirardini *et al.*, Opt. Lett. **42**, 559–562 (2017). Copyright 2017 Optical Society of America. Panel (k) reproduced with permission from Liu *et al.*, Nano Lett. **16**, 5426–5432 (2016). Copyright 2016 American Chemical Society. Panel (l) reproduced from Gili *et al.*, Beilstein J. Nanotechnol. **9**, 2306–2314 (2018) under Full Beilstein-Institut Open Access License Agreement 1.2. Panel (m) reproduced with permission from Renaut *et al.*, Nano Lett. **19**, 877–884 (2019). Copyright 2019 American Chemical Society. Panel (m) reproduced with permission from Linnenbank *et al.*, Light Sci. Appl. **5**, e16013 (2016). Copyright 2016 Springer Nature.

based nanoantennas relies in the enhancement of the Q factor by tuning the resonances of dielectric nanoantennas to the bound states in the continuum (BIC) formed via destructive interference of two similar leaky modes. Theoretically predicted in 2018 by means of an AlGaAs nanoantenna model for SHG enhancement by Carletti and co-workers (Carletti *et al.*, 2018) and extended to THG in 2019 (Carletti *et al.*, 2019a), this approach was only very recently confirmed experimentally (Koshelev *et al.*, 2020).

Another effective route to enhance the harmonic generation at the nanoscale consists in combining the field enhancements in plasmonic antennas with the large bulk nonlinearities of dielectric materials. This strategy, which allows to circumvent both the limitations imposed by the losses in metals and the low field enhancements in dielectrics, is based on hybrid plasmonic-dielectric nanoscale systems. Two research groups simultaneously applied this concept, where a plasmonic gap nanoantenna is employed to confine the impinging pump fields to the spatial location of individual nonlinear nanocrystals, to enhance their THG (Aouani *et al.*, 2014 and Metzger *et al.*, 2014) [see Figs. 3(e) and 3(f)]. A similar approach was employed to enhance the THG in Si nanodisks at coincidence with the anapole mode, i.e., a specific condition where the superposition of a toroidal and an electric dipole mode with a π-phase difference produces optical transparency and allow for high energy storage in the nanoparticle (Shibanuma *et al.*, 2017) [see Fig. 3(g)]. Enhanced nonlinear response is achieved through the efficient coupling of the pump field by means of a plasmonic ring antenna placed around the dielectric material. This concept can be successfully applied also to enhance SHG (Gili *et al.*, 2018) [see Fig. 3(l)].

Other relevant approaches to boost the SHG in noncentrosymmetric nanocrystals are based on either simple plasmonic-dielectric heterodimers (Renaut *et al.*, 2019) [see Fig. 3(m)] or more elaborated geometries based on asymmetric cross gap antennas featuring a double resonance surrounding the nonlinear crystal (Linnenbank *et al.*, 2016) [see Fig. 3(n)]. Although extremely promising, in hybrid systems the nanocrystal location and the alignment of its nonlinear axis are extremely critical and often require extremely demanding fabrication steps. A future development would be the fabrication of plasmonic nanoantennas on top of ultrathin nonlinear substrates of well-defined nonlinear axis orientation (Weber *et al.*, 2017). The sizeable field confinement in the nonlinear substrate, thanks to the relatively high refractive index of common nonlinear materials (e.g., $LiNbO_3$, $BaTiO_3$), along with the strong field enhancements achievable in plasmonic gap antennas would largely prevail on the nonlinear background from the substrate bulk.

As mentioned in Sec. III, an intriguing solution for harmonic generation at the nanoscale resides in 2D materials, thanks to their unique band structure (Cox *et al.*, 2017 and Yoshikawa *et al.*, 2017). In particular, while THG conversion efficiency has been already characterized in single layer graphene (Kumar *et al.*, 2013), it has been recently shown that THG can be sizably enhanced by doping the system through external gating (Soavi *et al.*, 2018), opening up further perspectives in the possibility of electrically tailoring the nonlinear response at the nanoscale.

Thus far, we limited our discussion to individual nanoantennas and materials whose dimensions are confined below the diffraction limit of light, where the nonlinear emission often emerges from subwavelength hot spots. Subwavelength nonlinear emitters are indeed of utmost importance to attain the highest level of integration for application as active optical logic elements in all-optical communication networks. The record conversion efficiencies attained with dielectric and hybrid nanostructures, which exceed 10^{-5} for both SHG (Gili *et al.*, 2016) and THG (Shibanuma *et al.*, 2017), allow picturing these platforms as ideal candidates for perspective applications in parametric conversion and photon-by-photon logic operation at the nanoscale. Here, the low photon yields compared to typical nanoscale single photon sources, such as single molecules and quantum dots, could be easily mitigated by the low damage thresholds, the higher photostability and the room-temperature operation. In this framework, it was recently demonstrated for the first time a source of entangled photon pairs based on a nanoscale AlGaAs platform, which works at room temperature and can be integrated in silicon-compatible devices (Marino *et al.*, 2019a).

B. Enhanced harmonics generation and manipulation with nonlinear metasurfaces

Despite the large nonlinearities in terms of susceptibilities reported for nanoscale antennas, extreme integration comes at the expenses of the absolute conversion efficiency, which is hindered by the small volume of the active material and the impossibility of applying phase matching conditions. In this framework, the ability of realizing nonlinear metasurfaces, where the nonlinear emission of individual efficient nanoantennas (i.e., nonlinear meta-atoms) is combined with collective interactions, allows achieving an improved efficiency along with new optical functionalities (Yu *et al.*, 2015 and Krasnok *et al.*, 2018). Optical metasurfaces are engineered 2D ensembles of ordered (Lin *et al.*, 2014 and Zheng *et al.*, 2015) or disordered (Jang *et al.*, 2018) sub-diffraction objects (i.e., meta-atoms) with tailored optical properties and constitute the basis for future ultraflat photonics. By carefully tailoring the interaction between meta-atoms, it has been shown that metasurfaces can provide superior and unprecedented optical functionalities (Khorasaninejad *et al.*, 2016), such as negative refraction (Yu *et al.*, 2011), compared to bulk optical elements, and in a much more compact realization. In this framework, metasurfaces of nonlinear nanoantennas have been shown to be an effective means to enhance and steer harmonic generation. A comprehensive overview on the perspective applications of nonlinear semiconductor metasurfaces was recently published by M. Shcherbakov and co-workers (Shcherbakov *et al.*, 2019). Here we will focus on the enhancement of harmonic generation provided by dielectric and hybrid metasurfaces.

To date, a plethora of nanoscale platforms that act as extremely efficient nonlinear meta-atoms are at hand. Although their size is obviously larger than the individual nonlinear oscillating dipoles (e.g., atoms, molecules, unitary cells) in nonlinear materials, these nanostructures have the potential to be engineered and arranged at will in planar geometries to further enhance the nonlinear optical effects [see Fig. 4(a)]. An efficient approach to engineer densely packed arrays of plasmonic nanoantennas consists in periodically arranging the nonlinear emitters to exploit the coherent nature of the nonlinear signal (Boardman and Zayatz, 2014 and Gentile *et al.*, 2011). The construct can be thought as the 2D equivalent of periodical poling, where instead a periodic inversion of the nanoantennas allows obtaining enhanced nonlinear emission in specific angular directions as a result of constructive interference of the nonlinear light [see Fig. 4(b)] (Segal *et al.*, 2015). The possibility of engineering the lattice modes of a periodic array of nanostructures to direct and beam the nonlinearly emitted light in preferential directions has been also recently applied by Marino *et al.* (2019b) to a purely dielectric metasurface. This result, combined with that published by the same group (Marino *et al.*, 2019a), allows envisioning the

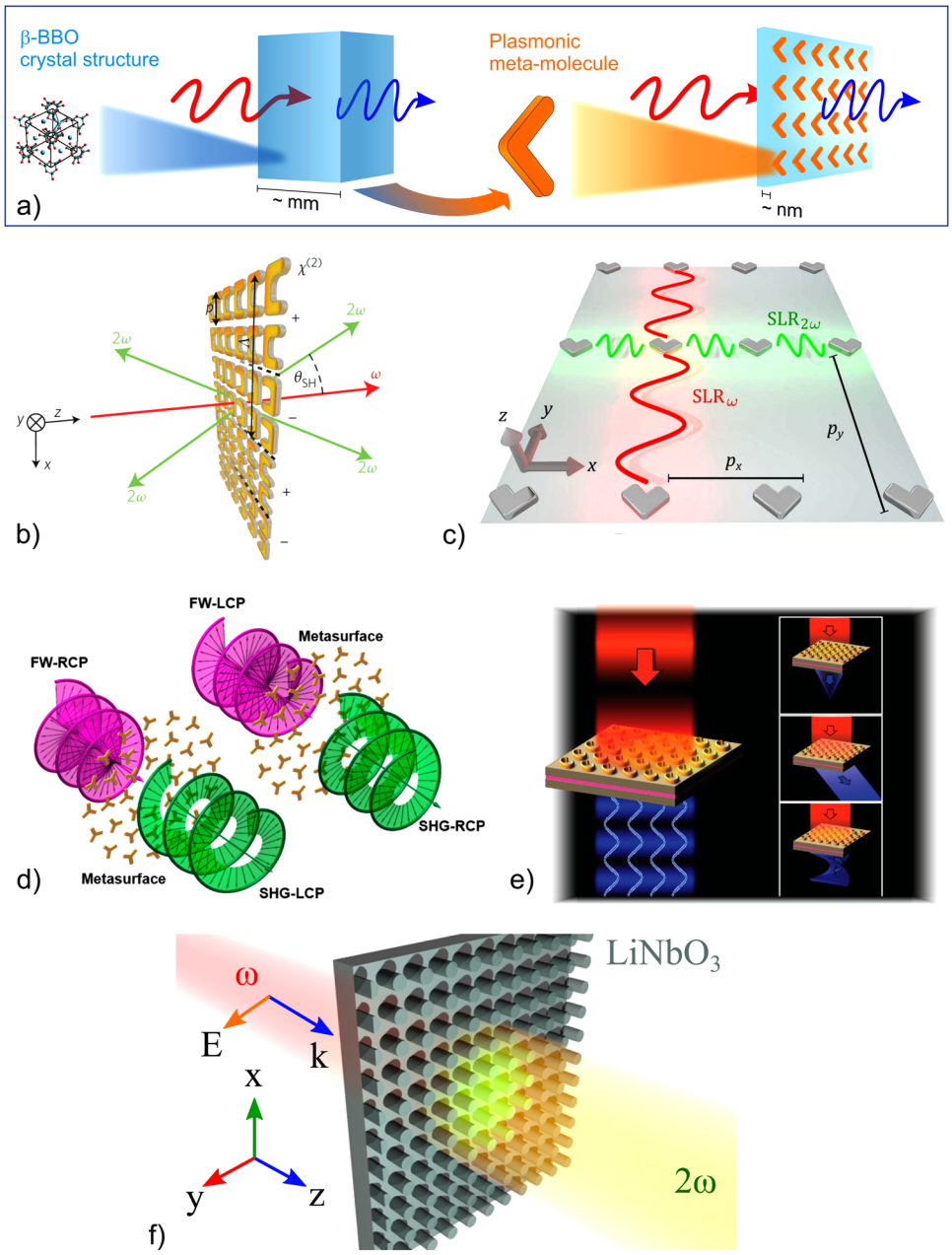

FIG. 4. Enhancement and steering of harmonic generation with nonlinear metasurfaces. (a) From bulk nonlinear crystals to nonlinear metasurfaces: a pictorial description. (b) An engineered periodically poled plasmonic metasurface to enhance and redirect SHG (Segal *et al.*, 2015). (c) A plasmonic metasurface that exploits surface lattice modes at both the pump and emission wavelength for the enhancement of the SHG (Huttunen *et al.*, 2019). (d) A plasmonic metasurface for the generation of nonlinear chiral light (Li *et al.*, 2017a; 2017b). (e) A plasmonic-dielectric hybrid metasurface for nonlinear light conversion, steering, and transformation (Wolf *et al.*, 2015). (f) A nanostructured $LiNbO_3$ crystal thin film for enhanced SHG proposed by Carletti and co-workers (Carletti, 2019b). Panel (b) reproduced with permission from Segal *et al.*, Nat. Photonics **9**, 180–184 (2015). Copyright 2015 Springer Nature. Panel (c) reproduced with permission from Huttunen *et al.*, J. Optics Soc. Am. B **36**, E30–E35 (2019). Copyright 2019 Optical Society of America. Panel (d) reproduced with permission from Li *et al.*, Nano Lett. **17**, 7974–7979 (2017). Copyright 2017 American Chemical Society. Panel (e) reproduced from Wolf *et al.*, Nat. Commun. **6**, 7667 (2015) under the terms of the Creative Commons CC BY license.

possibility of beaming entangled photons into very small angles. This is extremely attracting from a purely technological point of view, since it would allow one to efficiently couple entangled photons into low numerical aperture optical fibers.

A more intriguing approach suggested by Czaplicki and colleagues (Czaplicki *et al.*, 2016) consists in exploiting the lattice modes sustained by a less dense array of nonlinear nanoantennas. In this framework, it has been recently theoretically predicted an enhancement factor of about 10^6 with respect to an individual plasmonic nanoantenna, obtained when the array features active lattice modes at both the pump and emission wavelength as shown in Fig. 4(c) (Huttunen *et al.*, 2019).

The ability of engineering these nonlinear metasurface does not only allow one to push the limit of conversion efficiency but also to attain additional optical functionalities. For example, the generation of nonlinear chiral fields at the nanoscale (see Sec. III) has been recently transferred successfully into a metasurface device capable of generating nonlinear chiral fields [see Fig. 4(d)]

(Li *et al.*, 2017b), which in turn could be employed for encoding nonlinear images (Weber *et al.*, 2017). Finally, Fig. 4(e) shows plasmonic-semiconductor hybrid metasurfaces that have been applied for beam formation and nonlinear chiral light generation with record efficiency (Wolf *et al.*, 2015).

A future perspective for hybrid configurations, as already discussed in the previous paragraph, is the possibility of enhancing the nonlinear emission from a crystal using the field enhancements of plasmonic antennas fabricated on top of the crystal itself. A thin substrate made of a single non centrosymmetric crystal coupled with an engineered array of plasmonic antennas where the plasmonic lattice mode resonances are designed to enhance the pump field in the thin crystal as well as the emission of the nonlinearly excited dipoles in the crystal would indeed constitute a novel concept of nonlinear metasurface (Krasnok *et al.*, 2018). Hybrid metasurfaces obtained by coupling plasmonic nanohole arrays to 2D materials are also extremely promising to attain efficient focusing of the nonlinear light (Chen *et al.*, 2018). An interesting perspective of nonlinear metalenses is their potential exploitation in medical endoscopy (Lee *et al.*, 2020), to convert in situ a high-power infrared light into a focused beam in the visible range to perform local diagnosis or to be employed as optical tweezers in a non-invasive way.

To circumvent the limitations imposed by losses and low damage threshold in plasmonic antennas, another intriguing possibility resides in nanostructuring the surface of the crystal itself. Although the refractive index of the nanostructures would not show any discontinuity with respect to that of the substrate, which would be desirable to better confine the fields in the nanostructures, it has been theoretically demonstrated that this approach could lead to significant enhancement in the SHG from thin layers of $LiNbO_3$ [see Fig. 4(f)] Carletti *et al.*, 2019b). Enhanced nonlinear effects have been indeed already experimentally reported in the ultraviolet range by means of $BaTiO_3$ metasurfaces (Timpu *et al.*, 2019b).

A fundamental feature in plasmonic, photonic and hybrid metasurfaces featuring high nonlinear susceptibilities is the possibility to generate efficient frequency mixing under relaxed phase-matching conditions, which may enable a variety of applications. The Cluzel group recently demonstrated that plasmonic metasurfaces can be exploited as a saturable absorber in a laser cavity to realized Q-switching (Wang *et al.*, 2020). A perspective application for nonlinear metasurfaces is their implementation as intracavity frequency-converters in ultracompact laser cavities, e.g., in vertical-external-cavity surface-emitting-laser (VECSEL). They are also ideal candidates for realizing broadband frequency upconversion and downconversion in ultraflat devices, e.g., for converting thermal radiation in visible light in night vision goggles (Neshev *et al.*, 2018 and Morales *et al.*, 2019), and devising heralded photon sources based on SPDC for quantum optics (Wang *et al.*, 2018a; 2018b). Extended to the THz spectral region, the concept of nonlinear metasurfaces would allow to enrich the palette of sensors and coherent sources that are now available (Lee *et al.*, 2014). Finally, the enhanced nonlinear properties in metasurfaces could be exploited to further enhance the performances of sensing platforms with respect to those of simple dense arrays of nonlinear particles (Mesch *et al.*, 2016 and Ghirardini *et al.*, 2018), as we will describe in Sec. V.

V. HARMONIC GENERATION AS A TOOL FOR BIO-ORIENTED APPLICATIONS

Since the first nonlinear optical phenomena were reported in plasmonic nanostructures (Lippitz *et al.*, 2005), plasmon-enhanced nonlinear sensing has always been sought as a natural application for such phenomena. In fact, the nonlinear dependence on the illumination intensity and the inherent rejection of the pump light by spectral filtering are key features that can be exploited to surpass the sensitivity limits of linear sensing. A standard figure of merit in linear plasmonic sensing is the resonance maximum wavelength shift per unit of refractive index. In nonlinear plasmonic sensing, this figure of merit is not relevant. The relative change of intensity per unit of refractive index would seem the more appropriate figure to be employed given the nonlinear sensitivity of the mechanism to the environment. Following this concept, THG in nanoantenna arrays was the first to be tested as a probe in plasmon-enhanced nonlinear sensing (Mesch *et al.*, 2016), thanks to the relatively high THG yields in the visible range. Yet, as already discussed in Sec. III, the extreme surface sensitivity of plasmon-enhanced SHG makes it an appealing alternative for nonlinear sensing (Russier-Antoine *et al.*, 2008 and El Harfouch *et al.*, 2014). A preliminary study on engineered nanoantennas demonstrated that SHG-based plasmonic sensing can be at least as sensitive as the linear one despite the extremely low SHG yield (Ghirardini *et al.*, 2018). The current flourishing of plasmon-enhanced SHG sensing is testified by its recent application to the detection and orientation assessment of single molecules in nanohole arrays (Sahu *et al.*, 2019) and for the successful detection of picomolar concentrations of mercury in blood (Verma *et al.*, 2020). These first studies report sensitivities that only partially outperform those of the linear counterpart. In perspective, a significant enhancement of the sensitivity is expected through the implementation of more efficient platforms, such as optimized nanoantenna geometries (Celebrano *et al.*, 2015 and Gennaro *et al.*, 2016) or plasmonic and photonic metasurfaces engineered to feature collective modes and improved directionality of the outcoupled nonlinear radiation (Segal *et al.*, 2015; Huttunen *et al.*, 2019; and Marino *et al.*, 2019b) (see Sec. IV B). Thanks to the coherence of the processes, nonlinear signal—and hence sensitivity—can be further enhanced via an additional external seed beam (see Sec. VI). Therefore, although these first studies are still far from clinical applications, the availability of novel cheap ultrafast lasers sources working in the transparency window of tissues, the sensitivities attained thus far and the recent advances in nonlinear signal enhancement set the ground for a swift change in paradigm for nonlinear plasmonic sensing platforms in the next years.

In bio-imaging and bio-medical applications, the adoption of nanoparticles as labels is often motivated by one or more of their properties: (i) better photostability in comparison to dye molecules and fluorescent proteins, (ii) access to multimodal readout (e.g., optical and magnetic), and (iii) possibility to take advantage of additional physical properties (e.g., photothermal effect, selective accumulation in tumors), in some cases (iv) the possibility to apply multiplexed detection schemes. To date, most of the proposed imaging approaches are based on luminescent nanoparticles, such as semiconductor quantum dots, gold colloids, and upconversion nanoparticles. The use of harmonic generating nanostructures as

markers is still at its early stages of development, the main practical obstacle being the requirement of a pulsed femtosecond laser as light source. However, the increasing availability of rugged and cost-effective ultrafast sources working outside the classical Ti: Sapphire spectral region is progressively stimulating efforts in this direction. The main benefits of the harmonic approach for imaging can be summarized as:

(i) The inherent absence of bleaching and blinking, as only virtual states are involved in the harmonic process provided that the particles are excited out of their absorption bands (see Fig. 1).
(ii) Wide excitation/emission flexibility throughout the transparency range of the nanoparticle material.
(iii) Simultaneous emission at multiple harmonic orders with spectrally narrow bands.
(iv) Coherent and polarization-sensitive response.

The combination of properties (i) to (ii) provides a unique asset for applications requiring long-term monitoring of nanoparticle-labelled structures in optically congested samples, such as biological tissues. In particular, the possibility to tune the excitation towards longer wavelengths assumes a great significance in the light of the extended transparency windows in the infrared recently proposed: NIR-II (1100–1350 nm) and NIR-III (1600–1870 nm). These spectral regions correspond to local minima of water absorption at wavelengths beyond the classical transparency window (NIR-I, 650–950 nm). Although water absorption in these regions is comparatively higher than in NIR-I, the scattering efficiency is severely reduced and the overall light penetration in tissue is favored. For a comparison, Sordillo *et al.* have reported that the total attenuation length (a parameter closely related to the penetration of ballistic photons) is three-fold longer for NIR-III than in NIR-I for a healthy prostate tissue (600 μm vs 200 μm) although for other samples the difference is less significant (e.g., breast cancer) (Sordillo *et al.*, 2014). Notably, it has been demonstrated that working in these extended NIR windows allows performing multi-photon imaging in brain through the intact skull (Wang *et al.*, 2018a; 2018b). It is worth reminding that lower scattering along the excitation path which preserves the ballistic photon component is essential for the success of a nonlinear interaction where intensity, which depends both on the spatial and temporal structure of the pulse at the focal spot, plays a crucial role. On the other hand, in the detection path, scattering is less problematic as for scanning imaging techniques, the collection angle is large and even multiple scattered signal photons can be collected.

In most of the nonlinear imaging applications proposed to date, the detection of noble metal nanoparticles relies on their photoluminescence properties (especially for Au particles). Operation with harmonic emission (Lippitz *et al.*, 2005 and Tai *et al.*, 2007) is quite uncommon for plasmonic particles and substantially less exploited than in the case of bio-imaging by dielectric particles, where the harmonic approach has been pursued for silicon (Jung *et al.*, 2009) and for various metal oxides. A peculiar characteristic of non-centrosymmetric metal oxides, also known as Harmonic Nanoparticles (HNPs), is that the harmonic emission (and *a fortiori* the lowest even order, SHG) originates from the bulk rather than the surface, at least for diameters beyond 20 nm (Kim *et al.*, 2013). It follows that the nonlinear emission intensity scales as the volume squared, rendering rather large HNPs in the 50–150 nm range quite efficient as nonlinear biomarkers. HNPs have been applied *in vitro*, (Nakayama *et al.*, 2007) *ex vivo*, and *in vivo* (Pantazis *et al.*, 2010) over the years. An example of multiphoton imaging of a fluorescently stained zebrafish loaded with $BaTiO_3$ nanoparticles injected during its development is presented in Fig. 5.

A very recent development for imaging is the simultaneous collection of second and third harmonic upon NIR-II excitation at 1300 nm. This multi-order detection scheme is effective in increasing imaging selectivity by suppressing the hindrance from auto-fluorescence and from the harmonic background emitted by endogenous structures such as collagen (SHG) and lipids (THG) [see Fig. 6(a)] (Rogov *et al.*, 2015b and Dubreil *et al.*, 2017). The extended imaging penetration enabled by NIR-II and NIR-III combined with the sub-cellular spatial resolution proper to optical approaches (and not accessible to MRI, CT and other whole body imaging techniques) constitutes an undeniable asset for tracking individual cells, with straightforward applications for the assessment of regenerative therapies based on the engraftment of stem cells (Dubreil *et al.*, 2017) and for studies on immune-response reactions (Ramos-Gomes *et al.*, 2019).

Harmonic imaging presents other distinctive features when compared to fluorescence imaging, for instance because of the phase-coherent nature of the collected signals. In fact, the interferences taking place among the emissions stemming from multiple harmonic objects in a sub-diffraction limited spot should be properly considered to compute the actual spatial resolution and the optical transfer function of the set-up [see Fig. 6(b)], which will differ from the classical (incoherent) case. The Psaltis and Depeursinge groups independently demonstrated that, by measuring the interference with respect to a reference second-harmonic field, the axial localization of a $BaTiO_3$ HNP embedded in a biological medium could be determined in a scan-less fashion with applications for object tracking in three dimensions (Hsieh *et al.*, 2009 and Shaffer *et al.*, 2010). The Ameloot group has addressed the field of fluorescence correlation spectroscopy/microscopy and developed a theoretical model accounting for the coherent intensity fluctuations of second harmonic objects diffusing in the focal volume of a laser (Slenders *et al.*, 2015). They successfully applied

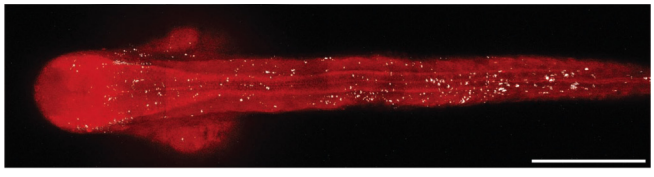

FIG. 5. Image of a fluorescently stained living zebrafish. The bright white spots correspond to the SHG emitted by $BaTiO_3$ nanoparticles (100–200 nm) with the poly(ethylene glycol) protected surface. The nanoparticles were injected into zygote-stage zebrafish embryos and persisted until the end of the development. Scale bar 300 μm. Image reprinted with permission from Culic-Viskota *et al.*, Nat. Protocols **7**, 1618–1633 (2012). Copyright 2012 Springer Nature.

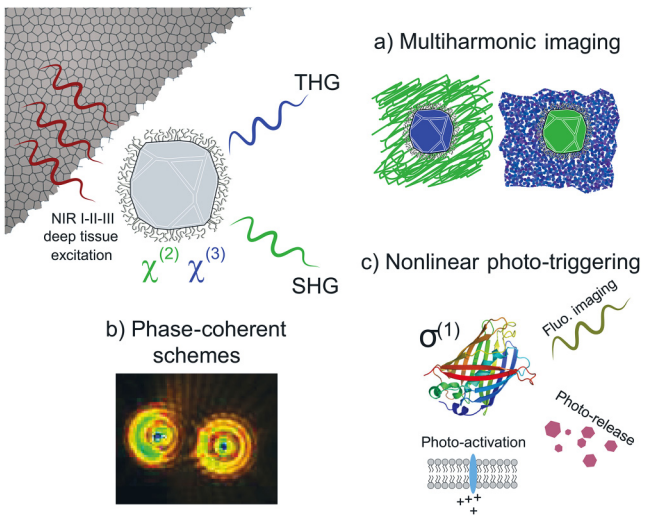

FIG. 6. Photo-interaction schemes enabled by harmonic nanoparticles embedded in a biological tissue. Efficient SHG and THG is obtained thanks to the high $\overleftrightarrow{\chi}^{(2)}$ and $\overleftrightarrow{\chi}^{(3)}$ values of the employed nanoparticles and the excitation at long wavelengths in the NIR-I-II-III windows, where light penetrates deeper in tissues because of reduced scattering and spectral minima in water absorption. (a) The simultaneous collection of SHG and THG allows differentiating the harmonic signal due to the nanoparticles from the one generated by endogenous structures (SHG collagen, THG lipids). Auto-fluorescence is minimal because of the long-wavelength excitation. (b) Contrary to fluorescence, the phase relationship between the fundamental and the harmonic emissions convey information (e.g., axial position) which can be retrieved by interferometric schemes. (c) The nanoparticle can efficiently convert NIR I-II-III radiation into UV and visible light *in situ*. Such emission can be prospectively used to excite nearby fluorescent proteins, to photo-release a drug or to activate a membrane protein in optogenetic procedures.

this model to study the mobility of $LiNbO_3$ 50 nm nanoparticles in human cells. Notably, they were able to quantify the diffusion coefficient from a single spectroscopy measurement without the need of external reference calibration (Slenders *et al.*, 2018).

In the case of dielectric nanoparticles, as the harmonic intensity depends on the elements of the nonlinear susceptibility tensor stimulated by the excitation field, the polarization analysis of the emission provides access to the orientation of the crystallographic axes of individual nanoparticle. This approach has been exploited over the years by several groups to distinguish small aggregates from mono-crystalline objects (Brasselet *et al.*, 2004). Recently, Brasselet and Grange have shown that polarization-resolved microscopy provides access to sub-diffraction limited information and they unraveled the crystalline heterogeneity at the surface of single $BaTiO_3$ HNP (Rendon-Barraza *et al.*, 2019). The advantages of polarization-resolved harmonic emission have been demonstrated also for bio-oriented applications. Macias-Romero and co-workers used this observable for quantifying the rotational diffusion properties of nanoparticles uptaken by cells, monitoring their dynamics at 50 μs frame rate. Such high imaging speed was obtained by focusing the output of a 200 kHz laser onto a large spot area and acquiring the second harmonic images in a wide-field fashion (Macias-Romero *et al.*, 2014). A different approach was pursued by Liu and collaborators who developed a polarization-sensitive superlocalization microscopy procedure. In their approach, the essential assumption common to all localization strategies (such as PALM or STORM) of having a single emitter active at a given time in the diffraction limited spot was based, rather than on bleaching or blinking, on the different SHG intensity profile of randomly oriented particles as a function of the varying linear polarization of the excitation laser. This way, the authors reported particle localization with 30 nm resolution based on Gaussian fitting of their spatially resolved emission. This sub-diffraction limited resolution allowed the quantification of overexpressed mRNA in cells tagged with properly labelled $BaTiO_3$ nanocrystals (Liu *et al.*, 2014).

Very recently, Malkinson *et al.* have demonstrated the use of KTP and BaTiO3 nanoparticles as imaging probes in the blood flow of a zebrafish model (Malkinson *et al.*, 2020). The originality of this study lies in the use of a multiphoton-light sheet microscope. In a series of well-designed experiments, the authors show that the presence of nondiagonal elements in the $\overleftrightarrow{\chi}^{(2)}$ tensor of a material is advantageous to enhance signal acquisition in the orthogonal detection.

The works reviewed in this section testify the liveliness of the field of harmonic-nanostructure imaging. Despite the exciting potential of the approach, these remain to-date proof-of-concept demonstrations. One must be aware that harmonic imaging markers cannot compete with luminescent nanoparticles in terms of brightness and widespread accessibility of the necessary experimental requirements. A key to their success relies on the ability of researchers in physics to identify the specific niches where this approach can be competitive and highlight to the life-science community the advantages of harmonic emission in terms of better imaging penetration and higher selectivity against background, for instance, exploiting their flexible spectral properties. Besides, letting aside the vast literature on metal NPs, several works have highlighted the low *in vitro* cytotoxicity of various metal-oxide particles used as harmonic probes in selected biological systems (Hsieh *et al.*, 2009; Staedler *et al.*, 2015; Li *et al.*, 2016; Dubreil *et al.*, 2017; and Sugiyama *et al.*, 2018) and also identified some exceptions (Staedler *et al.*, 2012). In general, because of the lack of heavy metals in the composition of many metal-oxide NPs, they might be preferred to quantum dots containing Hg or Cd. However, we emphasize that it is not possible to provide a general assessment in this respect as cytotoxicity and—*a fortiori*—biocompatibility of nanoparticles critically depends on their size, shape, surface modification, concentration, uptake mechanisms involved, and cell lines tested (Albanese *et al.*, 2012). The volume squared dependence of signal intensity (at least for bulk harmonic generation) implies that the particles used for imaging are rather large (30–100 nm) compared to other approaches (quantum dots 10 nm, upconversion nanoparticles 20 nm), therefore these markers should be more efficiently employed for cell tracking applications over extended time periods, taking advantage of their inherent photostability, rather than for intracellular studies where smaller size is often an essential requirement. Most of the metal-oxide synthesis protocols, although very cost-effective, result in rather large size- and morphology-dispersed samples. In terms of control of these parameters, nonlinear metal nanoparticles present clear advantages.

In the near future, we will likely witness a flourishing of imaging protocols based on phase-coherent detection schemes. In particular, the coherent nature of the process can be exploited to amplify the signal by means of either an external local oscillator or a seed beam in a homodyne-like or stimulated configuration. Apart from coherent-amplification procedures, which will be detailed in Sec. VI, holography-type approaches by means of an external phase-reference may allow obtaining spatial information along the propagation axis in a scan-less fashion, thus increasing the volume imaging speed. Another and yet unexplored possibility could rely on the full recovery of the spectral phase of large bandwidth pulses (Extermann *et al.*, 2008) interacting with biological samples, exploiting the particle harmonic emission as a proxy. This method could in principle provide access to spatially resolved information about the optical properties of the sample (complex refractive index and dispersion properties). More importantly, the analysis of the coherent image formation can be potentially exploited to infer information on sub-diffraction features in nanostructures as reported in Fig. 2 (Duboisset *et al.*, 2019). This approach might be extended to investigate structural properties of endogenous harmonophores, as demonstrated by a recent study on the organization of microtubules in the cell cytoskeleton, which can be used to study the effects of microtubule-targeting drugs and to detect conformational changes in tubulin during neuronal maturation connected to the onset of degenerative diseases (Van Steenbergen *et al.*, 2019).

In situ nonlinear photo-triggering by UV and visible emission of harmonic particles upon NIR-I, II, III excitation could also be an enabling evolution of the field, relying on the high nonlinear conversion efficiency, in particular for particle sizes of the order of 100 nm. Very recently, two works have provided proof-of-principle demonstrations of the therapeutic integration of this scheme. In a first embodiment, the SHG emission from $BaTiO_3$ HNPs upon irradiation at 1040 nm resulted in the excitation of nearby photosensitizers (rose Bengal) used in photodynamic therapy (Sun *et al.*, 2019). In a second setting, the SHG emitted by Bismuth Ferrite nanoparticles was used as a stimulus to trigger the photo-uncaging of a molecular cargo (tryptophan) (Vuilleumier *et al.*, 2019) [see Fig. 6(c)]. Within this nonlinear photo-triggering approach, the tunability of harmonic generation in structures smaller than the coherence length can provide an efficient decoupling between the therapeutic photo-interaction (photosensitizer activation, drug release) and the diagnostic (imaging) procedure, which can be safely performed at longer wavelengths. Following a similar line of thinking, visible photons generated by THG upon NIR-II excitation can be absorbed in a one-photon process by a close-by molecule with much smaller n-photon ($n \geq 3$) cross section. Molecules of interest would include many fluorescent proteins (GFP, RFP, etc.) and also channel-rhodopsin or other light-activated proteins used in optogenetics (Ao *et al.*, 2019).

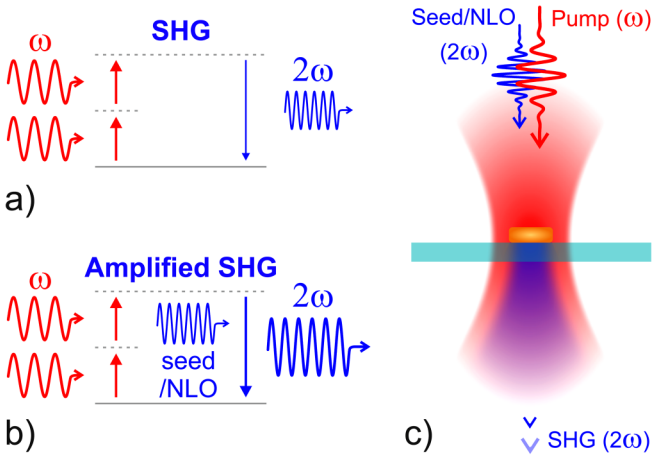

FIG. 7. Amplified SHG mechanism. Energy level scheme of standard (a) and amplified SHG (b) process. SHG amplification can be attained both in the homodyne-like configuration using an optical nonlinear local oscillator (NLO) and by stimulated effects using a seed beam. In both configurations, the amplifying beam is degenerate in energy with the emitted photons. (c) A sketch of the pump, seed/NLO and SHG signal beams at the sample.

VI. STRATEGIES TO AMPLIFY HARMONIC GENERATION FOR BIO-ORIENTED APPLICATIONS

As discussed in Sec. V, one of the most promising perspectives in label-assisted bioimaging using HNPs resides in the possibility to extend their operational wavelength to the extended NIR wavelength range. In particular, the fact that nonlinear optical processes do not involve resonant optical transitions in matter makes harmonic generation largely independent of the wavelength range. This constitutes, along with the absence of photobleaching, a major advantage with respect to common fluorophores, since these tags can be tracked within the transparency window of tissues. Still, to attain sizeable SHG yields, their sizes need to be larger than those of fluorescent labels, therefore they are expected to have limited interaction modalities and to remain confined to specific cell compartments once uptaken. The possibility of enhancing the SHG signal becomes therefore crucial, since it would allow one to considerably decrease the size of the HNPs and eventually enable even label-free NIR imaging of intracellular dynamics and in general of biological samples far from resonant optical transitions. An intriguing possibility is to exploit the coherent nature of nonlinear parametric processes to amplify them via heterodyne techniques (DeLange *et al.*, 1968) or by stimulated effects.

Homodyne-like interference has been effectively exploited in recent years to amplify the elastic scattering of nano-objects. Within this approach, where the scattering of the object is enhanced by the constructive interference with the light that is partially reflected by the substrate, which is exploited as a local oscillator (LO), it was possible to detect single quantum dots in their dark state (Kukura *et al.*, 2009) and even individual non-fluorescent molecules at room temperature (Celebrano *et al.*, 2011). In the nonlinear regime, this paradigm has been also applied to amplify SHG, exploiting a frequency-doubled external nonlinear LO (NLO) in an optical homodyne configuration (Yazdanfar *et al.*, 2004 and Le *et al.*, 2006) (see Fig. 7) and, very recently, extended to THG (Stock *et al.*, 2020). Interferometric amplification is an extremely versatile approach that does not rely on the optically active resonances in the sample or exogenous labels and could potentially benefit from further enhancements by exploiting resonances in

plasmonic nanoparticles employed as labels (Masia *et al.*, 2009 and Zhang *et al.*, 2016). Although interferometric amplification can be affected by phase decoherence and wavefront deformation, due to its sensitivity to the relative phase between the NLO and the signal and to the spatial overlap between their wavefronts, label-free imaging in biological samples via interferometric SHG has been recently reported in the visible range (Bancelin *et al.*, 2017). Stimulated processes were also reported as an attractive alternative to interferometry to amplify SHG (Goodman and Tisdale, 2015 and Gao *et al.*, 2018). Stimulated SHG allows performing amplification directly at the sample location. Therefore, compared to interferometric SHG, it is less sensitive to wavefront deformation, since the phase and the spatial modes of the stimulating beam (seed) and that of the SHG signal need to overlap only at the sample location, and can be potentially detected background-free by exploiting a non-collinear geometry for the SHG signal and the seed beams. In perspective, if successfully implemented in simple experimental realizations, these approaches would have a tremendous impact on some key applications in life- and material-sciences, such as nonlinear label-free bio-imaging (Campagnola *et al.*, 2003; Weigelin *et al.*, 2012; and Macias-Romero *et al.*, 2019), label-assisted imaging with harmonic particles (Pantazis, 2010 and Dubreil *et al.*, 2017), nonlinear molecular sensing (Mesch *et al.*, 2016 and Ghirardini *et al.*, 2018) and also nanoscale material characterization (Duboisset *et al.*, 2019). Indeed, external amplification would enable a dramatic decrease of the integration times and, hence, the observation of faster dynamics in biological environments with extremely long observation periods. In nonlinear sensing, amplification would also allow one to enhance by orders of magnitude the sensitivity and resolution, which are ultimately related to the overall signal yield in background-free conditions.

VII. CONCLUSIONS

We provided an overview of the most recent advances in harmonic generation at the nanoscale and framed it in the wider context embracing the efforts of the scientific community to enhance nonlinear optical processes at the nano- and meta-scale. In recent years, the field of nonlinear photonics in extremely confined volumes rapidly reached a mature stage and first applications have been already demonstrated or are within reach, offering a palette of future perspectives in many fields, ranging from nonlinear bioimaging and biosensing to material characterization and to the development of novel compact platforms for efficient photon conversion. Here, we stressed the potential impact of these recent scientific achievements for the characterization of nanoscale materials, such as nanoparticles and 2D materials. We also envisage the realization of novel efficient nonlinear integrated devices obtained by engineering individual nanoscale nonlinear sources in ultra-flat metasurfaces for light-by-light manipulation. We have also highlighted the fundamental role of harmonic generation enhancement to improve the performances of nonlinear optical sensing platforms as well as label-assisted and label-free imaging of biological tissues in the context of degenerative diseases (Macias-Romero *et al.*, 2019 and Van Steenbergen *et al.*, 2019) and tumors (Weigelin *et al.*, 2012; Tilbury *et al.*, 2015; Drifka *et al.*, 2016; and Natal *et al.*, 2018). While important challenges are still to be faced in order to circumvent the small conversion efficiencies in very small volumes, the latest achievements already set the stage to promising forthcoming applications.

ACKNOWLEDGEMENTS

M.F. and M.C. carried out this work in the framework of "NOMEN" project funded by MIUR in 2019 under the PRIN 2017 programme (Project No. 2017MP7F8F). P.-F.B acknowledges funding from the Agence Nationale de la Recherche (ANR) under Contract No. CE24-RACINE-2017.

DATA AVAILABILITY

Data sharing is not applicable to this article as no new data were created or analyzed in this study.

REFERENCES

Accanto, N. *et al.*, "Phase control of femtosecond pulses on the nanoscale using second harmonic nanoparticles," Light Sci. Appl. **3**, e143 (2014).

Albanese, A., Tang, P. S., and Chan, W. C. W., "The effect of nanoparticle size, shape, and surface chemistry on biological systems," Ann. Rev. Biomed. Eng. **14**, 1–16 (2012).

Ao, Y., Zeng, K., Yu, B., Miao, Y., Hung, W., Yu, Z., Xue, Y., Tan, T. T. Y., Xu, T., Zhen, M., Yang, X., Zhang, Y., and Gao, S., "An upconversion nanoparticle enables near infrared-optogenetic manipulation of the *C. elegans* motor circuit," ACS Nano **13**, 3373–3386 (2019).

Aouani, H., Rahmani, M., Navarro-Cía, M., and Maier, S. A., "Third-harmonic-upconversion enhancement from a single semiconductor nanoparticle coupled to a plasmonic antenna," Nat. Nanotechnol. **9**, 290–294 (2014).

Bachelier, G., Russier-Antoine, I., Benichou, E., Jonin, C., Del Fatti, N., Vallée, F., and Brevet, P.-F., "Fano profiles induced by near-field coupling in heterogeneous dimers of gold and silver nanoparticles," Phys. Rev. Lett. **101**, 197401 (2008).

Bancelin, S., Couture, C., Pinsard, M. *et al.*, "Probing microtubules polarity in mitotic spindles *in situ* using interferometric second harmonic generation microscopy," Sci. Rep. **7**, 6758 (2017).

Biagioni, P., Huang, J.-S., and Hecht, B., "Nanoantennas for visible and infrared radiation," Rep. Prog. Phys. **75**, 024402 (2012).

Black, L. J., Wiecha, P. R., Wang, Y., De Groot, C. H., Paillard, V., Girard, C., Muskens, O. L., and Arbouet, A., "Tailoring second-harmonic generation in single L-shaped plasmonic nanoantennas from the capacitive to conductive coupling regime," ACS Photonics **2**, 1592–1601 (2015).

Bloembergen, N. and Shen, Y. R., "Optical nonlinearities of a plasma," Phys. Rev. **141**, 298–305 (1966).

Boardman, A. D. and Zayats, A. V., "Nonlinear plasmonics," in *Handbook of Surface Science* (North-Holland, 2014), Vol. 4, pp. 329–347.

Boden, S. A., Moktadir, Z., Bagnall, D. M., Mizuta, H., and Rutt, H. N., "Focused helium ion beam milling and deposition," Microelectron. Eng. **88**, 2452–2455 (2011).

Bonaccorso, F. *et al.*, "Graphene photonics and optoelectronics," Nat. Photonics **4**, 611 (2010).

Bonacina, L., Mugnier, Y., Courvoisier, F., Le Dantec, R., Extermann, J., Lambert, Y., Boutou, V., Galez, C., and Wolf, J. P., "Polar $Fe(IO_3)_3$ nanocrystals as local probes for nonlinear microscopy," Appl. Phys. B **87**, 399–403 (2007).

Bouhelier, A., Beversluis, M., Hartschuh, A., and Novotny, L., "Near-field second-harmonic generation induced by local field enhancement," Phys. Rev. Lett. **90**, 13903 (2003).

Boyd, R. W., *Nonlinear Optics* (Academic Press, New York, 1984).

Brasselet, S., Le Floc'h, V., Treussart, F., Roch, J. F., Zyss, J., Botzung-Appert, E., and Ibanez, A., "*In situ* diagnostics of the crystalline nature of single organic nanocrystals by nonlinear microscopy," Phys. Rev. Lett. **92**, 207401 (2004).

Butet, J., Bachelier, G., Duboisset, J., Bertorelle, F., Russier-Antoine, I., Jonin, C., Benichou, E., and Brevet, P. F., "Three-dimensional mapping of single gold nanoparticles embedded in a homogeneous transparent matrix using optical second-harmonic generation," Opt. Express **18**, 22314 (2010a).

Butet, J., Brevet, P.-F., and Martin, O. J. F., "Optical second harmonic generation in plasmonic nanostructures: From fundamental principles to advanced applications," ACS Nano **9**, 10545–10562 (2015).

Butet, J., Duboisset, J., Bachelier, G., Russier-Antoine, I., Benichou, E., Jonin, C., and Brevet, P. F., "Optical second harmonic generation of single metallic nanoparticles embedded in a homogeneous medium," Nano Lett. **10**, 1717 (2010b).

Butet, J. and Martin, O. J. F., "Evaluation of the nonlinear response of plasmonic metasurfaces: Miller's rule, nonlinear effective susceptibility method, and full-wave computation," J. Opt. Soc. Am. B **33**, A8–A15 (2016).

Butet, J., Russier-Antoine, I., Jonin, C., Lascoux, N., Benichou, E., and Brevet, P. F., "Sensing with multipolar second harmonic generation from spherical metallic nanoparticles," Nano Lett. **12**, 1697 (2012).

Butet, J., Russier-Antoine, I., Jonin, C., Lascoux, N., Benichou, E., and Brevet, P. F., "Effect of the dielectric core and embedding medium on the second harmonic generation from plasmonic nanoshells: Tunability and sensing," J. Phys. Chem. C **117**, 1172–1177 (2013).

Campagnola, P. and Loew, L., "Second-harmonic imaging microscopy for visualizing biomolecular arrays in cells, tissues and organisms," Nat. Biotechnol. **21**, 1356–1360 (2003).

Carletti, L., Koshelev, K., De Angelis, C., and Kivshar, Y., "Giant nonlinear response at the nanoscale driven by bound states in the continuum," Phys. Rev. Lett. **121**, 033903 (2018).

Carletti, L., Kruk, S. S., Bogdanov, A. A., De Angelis, C., and Kivshar, Y., "High-harmonic generation at the nanoscale boosted by bound states in the continuum," Phys. Rev. Res. **1**, 023016 (2019a).

Carletti, L., Li, C., Sautter, J., Staude, I., De Angelis, C., Li, T., and Neshev, D. N., "Second harmonic generation in monolithic lithium niobate metasurfaces," Opt. Express **27**, 33391–33398 (2019b).

Celebrano, M., Kukura, P., Renn, A., and Sandoghdar, V., "Single-molecule imaging by optical absorption," Nat. Photonics **5**, 95–98 (2011).

Celebrano, M., Locatelli, A., Ghirardini, L., Pellegrini, G., Biagioni, P., Zilli, A., Wu, X. F., Grossmann, S., Carletti, L., De Angelis, R., Duò, L., Hecht, B., and Finazzi, M., "Evidence of cascaded third-harmonic generation in noncentrosymmetric gold nanoantennas," Nano Lett. **19**, 7013–7020 (2019).

Celebrano, M., Wu, X. F., Baselli, M., Großmann, S., Biagioni, P., Locatelli, A., De Angelis, C., Cerullo, G., Osellame, R., Hecht, B., Duò, L., Ciccacci, F., and Finazzi, M., "Mode matching in multiresonant plasmonic nanoantennas for enhanced second harmonic generation," Nat. Nanotechnol. **10**, 412–417 (2015).

Chemla, D. S. and Zyss, J., *Nonlinear Optical Properties of Organic Molecules and Crystals. 1 & 2* (Academic Press, New York, 1987).

Chen, C. K., Castro, A. R. B., and Shen, Y. R., "Surface-enhanced second harmonic generation," Phys. Rev. Lett. **46**, 145–148 (1981).

Chen, J., Wang, K., Long, H., Han, X., Hu, H., Liu, W., Wang, B., and Lu, P., "Tungsten disulfide–Gold nanohole hybrid metasurfaces for nonlinear metalenses in the visible region" Nano Lett. **18**, 1344–1350 (2018).

Clays, K. and Persoons, A., "Hyper-Rayleigh scattering in solution," Phys. Rev. Lett. **66**, 2980 (1991).

Collins, J. T., Rusimova, K. R., Hooper, D. C., Jeong, H.-H., Ohnoutek, L., Pradaux-Caggiano, F., Verbiest, T., Carbery, D. R., Fischer, P., and Valev, V. K., "First observation of optical activity in hyper-Rayleigh scattering," Phys. Rev. X **9**, 011024 (2019).

Cox, J., Marini, A., and de Abajo, F., "Plasmon-assisted high-harmonic generation in graphene," Nat. Commun. **8**, 14380 (2017.

Culic-Viskota, J., Dempsey, W. P., Fraser, S. E., and Pantazis, P., "Surface functionalization of barium titanate SHG nanoprobes for *in vivo* imaging in zebrafish," Nat. Protocols **7**, 1618–1633 (2012).

Czaplicki, R., Kiviniemi, A., Laukkanen, J., Lehtolahti, J., Kuittinen, M., and Kauranen, M., "Surface lattice resonances in second-harmonic generation from metasurfaces," Opt. Lett. **41**, 2684–2687 (2016).

Dean, J. J. and van Driel, H. M., "Graphene and few-layer graphite probed by second-harmonic generation: Theory and experiment," Phys. Rev. B **82**, 125411 (2010).

DeLange, O. E., "Optical heterodyne detection," IEEE Spectrum **5**, 77–85 (1968).

Dimitropoulos, D., Raghunathan, V., Claps, R., and Jalali, B., "Phase-matching and nonlinear optical processes in silicon waveguides," Opt. Express **12**, 149–160 (2004).

Drifka, C. R. *et al.*, "Comparison of picrosirius red staining with second harmonic generation imaging for the quantification of clinically relevant collagen fiber features in histopathology samples," J. Histochem. Cytochem. **64**, 519–529 (2016).

Duboisset, J. and Brevet, P. F., "Salt-induced long-to-short range orientational transition in water," Phys. Rev. Lett. **120**, 263001 (2018).

Duboisset, J. and Brevet, P. F., "Second-harmonic scattering-defined topological classes for nano-objects," J. Phys. Chem. C **123**, 25303–25308 (2019).

Dubreil, L., Leroux, I., Ledevin, M., Schleder, C., Lagalice, L., Lovo, C., Fleurisson, R., Passemard, S., Kilin, V., Gerber-Lemaire, S., Colle, M. A., Bonacina, L., and Rouger, K., "Multi-harmonic imaging in the second near-infrared window of nanoparticle-labeled stem cells as a monitoring tool in tissue depth," ACS Nano **11**, 6672–6681 (2017).

Eckardt, R. C., Masuda, H., Fan, Y. X., and Byer, R. L., "Absolute and relative nonlinear optical coefficients of KDP, KD*P, BaB_2O_4, $LiIO_3$, MgO:$LiNbO_3$, and KTP measured by phase-matched second-harmonic generation," IEEE J. Quantum Electron. **26**, 922–933 (1990).

Eisenthal, K. B., "Equilibrium and dynamic processes at interfaces by second harmonic and sum frequency generation," Ann. Rev. Phys. Chem. **43**, 627 (1992).

El Harfouch, Y., Benichou, E., Bertorelle, F., Russier-Antoine, I., Jonin, C., Lascoux, N., and Brevet, P. F., "Hyper-Rayleigh scattering from gold nanorods," J. Phys. Chem. C **118**, 609 (2014).

Extermann, J., Bonacina, L., Courvoisier, F., Kiselev, D., Mugnier, Y., Le Dantec, R., Galez, C., and Wolf, J.-P., "Nano-FROG: Frequency resolved optical gating by a nanometric object," Opt. Express **16**, 10405–10411 (2008).

Finazzi, M., Biagioni, P., Celebrano, M., and Duò, L., "Selection rules for second harmonic generation in nanoparticles," Phys. Rev. B **76**, 125414 (2007).

Franken, P. A., Hill, A. E., Peters, C. W., and Weinreich, G., "Generation of optical harmonics," Phys. Rev. Lett. **7**, 118 (1961).

Gao, Y., Goodman, A. J., Shen, P.-C., Kong, J., and Tisdale, W. A., "Phase-modulated degenerate parametric amplification microscopy," Nano Lett. **18**, 5001–5006 (2018).

Gennaro, S. D., Li, Y., Maier, S. A., and Oulton, R. F., "Double blind ultrafast pulse characterization by mixed frequency generation in a gold antenna," ACS Photonics **5**, 3166–3171 (2018).

Gennaro, S. D., Rahmani, M., Giannini, V., Aouani, H., Sidiropoulos, T. P. H., Navarro-Cía, M., Maier, S. A., and Oulton, R. F., "The interplay of symmetry and scattering phase in second harmonic generation from gold nanoantennas," Nano Lett. **16**, 5278–5285 (2016).

Gentile, M., Hentschel, M., Taubert, R., Guo, H., Giessen, H., and Fiebig, M., "Investigation of the nonlinear optical properties of metamaterials by second harmonic generation," Appl. Phys. B **105**, 149 (2011).

Ghirardini, L., Baudrion, A.-L., Monticelli, M., Petti, D., Biagioni, P., Duò, L., Pellegrini, G., Adam, P.-M., Finazzi, M., and Celebrano, M., "Plasmon-enhanced second harmonic sensing," J. Phys. Chem. C **122**, 11475–11481 (2018).

Ghirardini, L., Carletti, L., Gili, V., Pellegrini, G., Duò, L., Finazzi, M., Rocco, D., Locatelli, A., De Angelis, C., Favero, I., Ravaro, M., Leo, G., Lemaître, A., and Celebrano, M., "Polarization properties of second-harmonic generation in AlGaAs optical nanoantennas," Opt. Lett. **42**, 559–562 (2017).

Gili, V. F., Carletti, L., Locatelli, A., Rocco, D., Finazzi, M., Ghirardini, L., Favero, I., Gomez, C., Lemaître, A., Celebrano, M., De Angelis, C., and Leo, G., "Monolithic AlGaAs second-harmonic nanoantennas," Opt. Express **24**, 15965–15971 (2016).

Gili, V. F., Ghirardini, L., Rocco, D., Marino, G., Favero, I., Roland, I., Pellegrini, G., Duò, L., Finazzi, M., Carletti, L., Locatelli, A., Lemaître, A., Neshev, D. N., De Angelis, C., Leo, G., and Celebrano, M., "Metal–dielectric hybrid nanoantennas for efficient frequency conversion at the anapole mode," Beilstein J. Nanotechnol. **9**, 2306–2314 (2018).

Goodman, A. J. and Tisdale, W. A., "Enhancement of second-order nonlinear-optical signals by optical stimulation," Phys. Rev. Lett. **114**, 183902 (2015).

Göppert-Mayer, M., "Elementary processes with two quantum transitions," Ann. Phys. **401**, 273 (1931).

Grinblat, G., Li, Y., Nielsen, M. P., Oulton, R. F., and Maier, S. A., "Enhanced third harmonic generation in single germanium nanodisks excited at the anapole mode," Nano Lett. **16**, 4635–4640 (2016).

Hanke, T., Krauss, G., Träutlein, D., Wild, B., Bratschitsch, R., and Leitenstorfer, A., "Efficient nonlinear light emission of single gold optical antennas driven by few-cycle near-infrared pulses," Phys. Rev. Lett. **103**, 257404 (2009).

Harutyunyan, H., Volpe, G., Quidant, R., and Novotny, L., "Enhancing the nonlinear optical response using multifrequency gold-nanowire antennas," Phys. Rev. Lett. **108**, 217403 (2012).

Hong, S.-Y., Dadap, J. I., Petrone, N., Yeh, P.-C., Hone, J., and Osgood Jr., R. M., "Optical third-harmonic generation in graphene," Phys. Rev. X **3**, 021014 (2013).

Hsieh, C.-L., Grange, R., Pu, Y., and Psaltis, D., "Three-dimensional harmonic holographic microcopy using nanoparticles as probes for cell imaging," Optics Express **17**, 2880–2891 (2009).

Hsieh, C.-L. *et al.*, "Bioconjugation of barium titanate nanocrystals with immunoglobulin G antibody for second harmonic radiation imaging probes," Biomaterials **31**, 2272–2277 (2010).

Hsu, W.-T., Zhao, Z.-A., Li, L.-J., Chen, C.-H., Chiu, M.-H., Chang, P.-S., Chou, Y.-C., and Chang, W.-H., "Second harmonic generation from artificially stacked transition metal dichalcogenide twisted bilayers," ACS Nano **8**, 2951–2958 (2014).

Hubert, C., Billot, L., Adam, P.-M., Bachelot, R., Royer, P., Grand, J., Gindre, D., Dorkenoo, K. D., and Fort, A., "Role of surface plasmon in second harmonic generation from gold nanorods," Appl. Phys. Lett. **90**, 181105 (2007).

Huttunen, M. J., Reshef, O., Stolt, T., Dolgaleva, K., Boyd, R. W., and Kauranen, M., "Efficient nonlinear metasurfaces by using multiresonant high-Q plasmonic arrays," J. Opt. Soc. Am. B **36**, E30–E35 (2019).

Jang, M., Horie, Y., Shibukawa, A., Brake, J., Liu, Y., Mahsa Kamali, S., Arbabi, A., Ruan, H., Faraon, A., and Yang, C., "Wavefront shaping with disorder-engineered metasurfaces," Nat. Photonics **12**, 84–90 (2018).

Joulaud, C., Mugnier, Y., Djanta, G., Dubled, M., Marty, J.-C., Galez, C., Wolf, J.-P., Bonacina, L., and Le Dantec, R., "Characterization of the nonlinear optical properties of nanocrystals by hyper Rayleigh scattering," J. Nanobiotechnol. **11**, S8 (2013).

Jung, Y., Tong, L., Tanaudommongkon, A., Cheng, J.-X., and Yang, C., "*In vitro* and *in vivo* nonlinear optical imaging of silicon nanowires," Nano Lett. **9**, 2440–2444 (2009).

Kachynski, A. V., Kuzmin, A. N., Nyk, M., Roy, I., and Prasad, P. N., "Zinc oxide nanocrystals for nonresonant nonlinear optical microscopy in biology and medicine," J. Phys. Chem. C **112**, 10721–10724 (2008).

Kasel, T. W., Deng, Z., Mroz, A. M., Hendon, C. H., Butler, K. T., and Canepa, P., "Metal-free perovskites for non linear optical materials," Chem. Sci. **10**, 8187–8194 (2019).

Kauranen, M. and Zayats, A. V., "Nonlinear plasmonics," Nat. Photonics **6**, 737–748 (2012).

Khorasaninejad, M., Chen, W. T., Devlin, R. C., Oh, J., Zhu, A. Y., and Capasso, F., "Metalenses at visible wavelengths: Diffraction-limited focusing and subwavelength resolution imaging," Science **352**, 1190–1194 (2016).

Khurgin, J. B., "Graphene-a rather ordinary nonlinear optical material," Appl. Phys. Lett. **104**, 161116 (2014).

Kim, E., Steinbrück, A., Buscaglia, M. T., Buscaglia, V., Pertsch, T., and Grange, R., "Second-harmonic generation of single $BaTiO_3$ nanoparticles down to 22 nm diameter," ACS Nano **7**, 5343–5349 (2013).

Kleinman, D. A., "Nonlinear dielectric polarization in optical media," Phys. Rev. **126**, 1977 (1962).

Kolkowski, R., Petti, L., Rippa, M., Lafargue, C., and Zyss, J., "Octupolar plasmonic meta–molecules for nonlinear chiral watermarking at subwavelength scale," ACS Photonics **2**, 899–906 (2015).

Koppens, F. H. L., Chang, D. E., and García de Abajo, F. J., "Graphene plasmonics: A platform for strong light–matter interactions," Nano Lett. **11**, 3370–3377 (2011).

Koshelev, K., Kruk, S., Melik-Gaykazyan, E., Choi, J.-H., Bogdanov, A., Park, H.-G., and Kivshar, Y., "Subwavelength dielectric resonators for nonlinear nanophotonics," Science **367**, 288–292 (2020).

Krasnok, A., Tymchenko, M., and Alù, A., "Nonlinear metasurfaces: A paradigm shift in nonlinear optics," Mater. Today **21**, 1–100 (2018).

Kukura, P., Celebrano, M., Renn, A., and Sandoghdar, V., "Imaging a single quantum dot when it is dark," Nano Lett. **9**, 926–929 (2009).

Kumar, N., Kumar, J., Gerstenkorn, C., Wang, R., Chiu, H.-Y., Smirl, A. L., and Zhao, H., "Third harmonic generation in graphene and few-layer graphite films," Phys. Rev. B **87**, 121406(R) (2013).

Kurtz, S. K. and Perry, T. T., "A powder technique for the evaluation of nonlinear optical materials," J. Appl. Phys. **39**, 3798 (1968).

Kuznetsov, A. I., Miroshnichenko, A. E., Brongersma, M. L., Kivshar, Y. S., and Luk'yanchuk, B., "Optically resonant dielectric nanostructures," Science **354**, aag2472 (2016).

Le, X. L., Brasselet, S., Treussart, F., Roch, J.-F., Marquier, F., Chauvat, D., Perruchas, S., Tard, C., and Gacoin, T., "Balanced homodyne detection of second-harmonic generation from isolated subwavelength emitters," Appl. Phys. Lett. **89**, 121118 (2006).

Le, X. L., Zhou, C., Slablab, A., Chauvat, D., Tard, C., Perruchas, S., Gacoin, T., Villeval, P., and Roch, J. F., "Photostable second-harmonic generation from a single $KTiOPO_4$ nanocrystal for nonlinear microscopy," Small **4**, 1332–1336 (2008).

Lee, D., Gwak, J., Badloe, T., Palomba, S., and Rho, J., "Metasurfaces-based imaging and applications: from miniaturized optical components to functional imaging platforms," Nanoscale Adv. **2**, 605–625 (2020).

Lee, J. *et al.*, "Giant nonlinear response from plasmonic metasurfaces coupled to intersubband transitions," Nature **511**, 65–69 (2014).

Li, G. *et al.*, "Nonlinear metasurface for simultaneous control of spin and orbital angular momentum in second harmonic generation," Nano Lett. **17**, 7974–7979 (2017a).

Li, G., Zhang, S., and Zentgraf, T., "Nonlinear photonic metasurfaces," Nat. Rev. Mater. **2**, 17010 (2017b).

Li, J. *et al.*, "Cellular internalization of $LiNbO_3$ nanocrystals for second harmonic imaging and the effects on stem cell differentiation," Nanoscale **8**, 7416–7422 (2016).

Li, Y., Rao, Y., Mak, K. F., You, Y., Wang, S., Dean, C. R., and Heinz, T. F., "Probing symmetry properties of few-layer MoS_2 and h-BN by optical second harmonic generation," Nanoletters **13**, 3329–3333 (2013).

Lin, D., Fan, P., Hasman, E., and Brongersma, M. L., "Dielectric gradient metasurface optical elements," Science **345**, 298–302 (2014).

Linnenbank, H., Grynko, Y., Förstner, J., and Linden, S., "Second harmonic generation spectroscopy on hybrid plasmonic/dielectric nanoantennas," Light Sci. Appl. **5**, e16013 (2016).

Lippitz, M., van Dijk, M. A., and Orrit, M., "Third-harmonic generation from single gold nanoparticles," Nano Lett. **5**, 799–802 (2005).

Liu, J., Cho, I.-H., Cui, Y., and Irudayaraj, J., "Second harmonic super-resolution microscopy for quantification of mRNA at single copy sensitivity," ACS Nano **8**, 12418–12427 (2014).

Liu, S., Sinclair, M. B., Saravi, S., Keeler, G. A., Yang, Y., Reno, J., Peake, G. M., Setzpfandt, F., Staude, I., Pertsch, T., and Brener, I., "Resonantly enhanced

second-harmonic generation using III−V semiconductor all-dielectric metasurfaces," Nano Lett. **16**, 5426–5432 (2016).
Liu, S., Vabishchevich, P. P., Vaskin, A., Reno, J. L., Keeler, G. A., Sinclair, M. B., Staude, I., and Brener, I., "An all-dielectric metasurface as a broadband optical frequency mixer," Nat. Commun. **9**, 2507 (2018).
Macias-Romero, C., Didier, M. E., Zubkovs, V., Delannoy, L., Dutto, F., Radenovic, A., and Roke, S., "Probing rotational and translational diffusion of nanodoublers in living cells on microsecond time scales," Nano Lett. **14**, 2552–2557 (2014).
Macias-Romero, C., Teulon, C., Didier, M., and Roke, S., "Endogenous SHG and 2PEF coherence imaging of substructures in neurons in 3D," Opt. Express **27**, 2235–2247 (2019).
Maiman, T., "Stimulated optical radiation in ruby," Nature **187**, 493 (1960).
Majérus, B. *et al.*, "Optical second harmonic generation from nanostructured graphene: A full wave approach," Opt. Express **25**, 27015–27027 (2017).
Malard, L. M., Alencar, T. V., Barboza, A. P. M., Mak, K. F., and de Paula, A. M., "Observation of intense second harmonic generation from MoS_2 atomic crystals," Phys. Rev. B **87**, 201401(R) (2013).
Malkiel, I., Mrejen, M., Nagler, A. *et al.*, "Plasmonic nanostructure design and characterization via Deep Learning," Light Sci. Appl. **7**, 60 (2018).
Malkinson, G., Mahou, P., Chaudan, E., Gacoin, T., Sonay, A., Pantazis, P., Beaurepaire, E., and Supatto, W., "Fast *in vivo* imaging of SHG nanoprobes with multiphoton light-sheet microscopy," ACS Photonics **7**, 1036–1049 (2020).
Manzeli, S., Ovchinnikov, D., Pasquier, D., Yazyev, O. V., and Kis, A., "2D transition metal dichalcogenides," Nat. Rev. Mater. **2**, 17033 (2017).
Marino, G., Gigli, C., Rocco, D., Lemaître, A., Favero, I., De Angelis, C., and Leo, G., "Zero-order second harmonic generation from AlGaAs-on-insulator metasurfaces," ACS Photonics **6**, 1226–1231 (2019b).
Marino, G. *et al.*, "Spontaneous photon-pair generation from a dielectric nanoantenna," Optica **6**, 1416–1422 (2019a).
Masia, F., Langbein, W., Watson, P., and Borri, P., "Resonant four-wave mixing of gold nanoparticles for three-dimensional cell microscopy," Opt. Lett. **34**, 1816–1818 (2009).
Mayer, L. *et al.*, "Single KTP nanocrystals as second-harmonic generation biolabels in cortical neurons," Nanoscale **5**, 8466–8471 (2013).
Mennel, L., Paur, M., and Mueller, T., "Second harmonic generation in strained transition metal dichalcogenide monolayers: MoS_2, $MoSe_2$, WS_2, and WSe_2," APL Photonics **4**, 034404 (2018).
Mesch, M., Metzger, B., Hentschel, M., and Giessen, H., "Nonlinear plasmonic sensing," Nano Lett. **16**, 3155–3159 (2016).
Metzger, B., Hentschel, M., Schumacher, T., Lippitz, M., Ye, X., Murray, C. B., Knabe, B., Buse, K., and Giessen, H., "Doubling the efficiency of third harmonic generation by positioning ITO nanocrystals into the hot-spot of plasmonic gap-antennas," Nano Lett. **14**, 2867–2872 (2014).
Morales, M. C., "Infrared imaging in nonlinear GaAs metasurfaces," SPIE Micro + Nano Mater. Devices Appl. **11201**, 112011S (2019).
Naik, G. V., Shalaev, V. M., and Boltasseva, A., "Alternative plasmonic materials: Beyond gold and silver," Adv. Mat. **25**, 3264–3294 (2013).
Nakayama, Y., Pauzauskie, P. J., Radenovic, A., Onorato, R. M., Saykally, R. J., Liphardt, J., and Yang, P., "Tunable nanowire nonlinear optical probe," Nature **447**, 1098–1101 (2007).
Nappa, J., Revillod, G., Russier-Antoine, I., Benichou, E., Jonin, C., and Brevet, P. F., "Electric dipole origin of the second harmonic generation of small metallic particles," Phys. Rev. B **71**, 165407 (2005).
Natal, R. A. *et al.*, "Collagen analysis by second-harmonic generation microscopy predicts outcome of luminal breast cancer," Tumor Biol. **40**, 1–12 (2018).
Neshev, D. and Aharonovich, I., "Optical metasurfaces: New generation building blocks for multi-functional optics," Light Sci. Appl. **7**, 58 (2018).
Niederberger, M. *et al.*, "A general soft-chemistry route to perovskites and related materials: Synthesis of $BaTiO_3$, $BaZrO_3$, and $LiNbO_3$ nanoparticles," Angew. Chem. **43**, 2270–2273 (2004).
Novotny, L. and Van Hulst, N. F., "Antennas for light," Nat. Photonics **5**, 83–90 (2011).
Nye, J. F., *Physical Properties of Crystals* (Clarendon, Oxford, 1957).
O'Brien, K., Suchowski, H., Rho, J. *et al.*, "Predicting nonlinear properties of metamaterials from the linear response," Nat. Mater. **14**, 379–383 (2015).
Pantazis, P., Maloney, J., Wu, D., and Fraser, S. E., "Second harmonic generating (SHG) nanoprobes for *in vivo* imaging," Proc. Natl. Acad. Sci. U,S.A.. **107**, 14535–14540 (2010).
Pu, Y., Grange, R., Hsieh, C.-L., and Psaltis, D., "Nonlinear optical properties of core-shell nanocavities for enhanced second-harmonic generation," Phys. Rev. Lett. **104**, 207402 (2010).
Ramos-Gomes, F., Möbius, W., Bonacina, L., Alves, F., and Markus, M. A., "Bismuth ferrite second harmonic nanoparticles for pulmonary macrophage tracking," Small **15**, 1970024 (2019).
Renaut, C., Lang, L., Frizyuk, K., Timofeeva, M., Komissarenko, F. E., Mukhin, I. S., Smirnova, D., Timpu, F., Petrov, M., Kivshar, Y., and Grange, R., "Reshaping the second-order polar response of hybrid metal− dielectric nanodimers," Nano Lett. **19**, 877–884 (2019).
Rendón-Barraza, C., Timpu, F., Grange, R., and Brasselet, S., "Crystalline heterogeneity in single ferroelectric nanocrystals revealed by polarized nonlinear microscopy," Sci. Rep. **9**, 1670 (2019).
Riporto, J. *et al.*, "Second harmonic spectroscopy of ZnO, $BiFeO_3$ and $LiNbO_3$ nanocrystals," Opt. Mater. Express **9**, 1955–1966 (2019).
Riporto, J., Demierre, A., Kilin, V., Balciunas, T., Schmidt, C., Campargue, G., Urbain, M., Baltuska, A., Le Dantec, R., Wolf, J.-P., and Bonacina, L., "Bismuth ferrite dielectric nanoparticles excited at telecom wavelengths as multicolor sources by second, third, and fourth harmonic generation," Nanoscale **10**, 8146–8152 (2018).
Rogov, A., Irondelle, M., Ramos Gomes, F., Bode, J., Staedler, D., Passemard, S., Courvoisier, S., Yamamoto, Y., Waharte, F., Ciepielewski, D., Rideau, P., Gerber-Lemaire, S., Alves, F., Salamero, J., Bonacina, L., and Wolf, J.-P., "Simultaneous multiharmonic imaging of nanoparticles in tissues for increased selectivity," ACS Photonics **2**, 1416–1422 (2015a).
Rogov, A., Mugnier, Y., and Bonacina, L., "Harmonic nanoparticles: Noncentrosymmetric metal oxides for nonlinear optics," J. Optics **17** (2015b).
Russier-Antoine, I., Benichou, E., Bachelier, G., Jonin, C., and Brevet, P.-F., "Multipolar contributions of the second harmonic generation from silver and gold nanoparticles," J. Phys. Chem. C **111**, 9044–9048 (2007).
Russier-Antoine, I., Fakhouri, H., Basu, S., Bertorelle, F., Dugourd, P., Brevet, P.-F., Velayudhan, P., Thomas, S., Kalarikkal, N., and Antoine, R., "Second harmonic scattering from mass characterized 2D graphene oxide sheets," Chem. Commun. **56**, 3859–3862 (2020).
Russier-Antoine, I., Huang, J., Benichou, E., Bachelier, G., Jonin, C., and Brevet, P. F., "Hyper Rayleigh scattering of protein-mediated gold nanoparticles aggregates," Chem. Phys. Lett. **450**, 345 (2008).
Sahu, P. S., Mahigir, A., Chidester, B., Veronis, G., and Gartia, M. R., "Ultrasensitive three-dimensional orientation imaging of single molecules on plasmonic nanohole arrays using second harmonic generation," Nano Lett. **19**, 6192–6202 (2019).
Schuller, J. A., Barnard, E. S., Cai, W., Jun, Y., White, J. S., and Brongersma, M., "Plasmonics for extreme light concentration and manipulation," Nat. Mater. **9**, 193–204 (2010).
Schwung, S. *et al.*, "Nonlinear optical and magnetic properties of $BiFeO_3$ harmonic nanoparticles," J. Appl. Phys. **116**, 114306 (2014).
Segal, N., Keren-Zur, S., Hendler, N., and Ellenbogen, T., "Controlling light with metamaterial-based nonlinear photonic crystals," Nat. Photonics **9**, 180–184 (2015).
Shaffer, E., Marquet, P., and Depeursinge, C., "Real time, nanometric 3D-tracking of nanoparticles made possible by second harmonic generation digital holographic microscopy," Opt. Express **18**, 17392–17403 (2010).
Shcherbakov, M. R., Eilenberger, F., and Staude, I., "Interaction of semiconductor metasurfaces with short laser pulses: From nonlinear optical response toward spatiotemporal shaping," J. Appl. Phys. **126**, 085705 (2019).
Shcherbakov, M. R., Neshev, D. N., Hopkins, B., Shorokhov, A. S., Staude, I., Melik-Gaykazyan, E. V., Decker, M., Ezhov, A. A., Miroshnichenko, A. E.,

Brener, I., Fedyanin, A. A., and Kivshar, Y. S., "Enhanced third-harmonic generation in silicon nanoparticles driven by magnetic response," Nano Lett. **14**, 6488–6492 (2014).
Shen, Y. R., "Optical second harmonic generation at interfaces," Ann. Rev. Phys. Chem. **40**, 327–350 (1989).
Shibanuma, T., Grinblat, G., Albella, P., and Maier, S. A., "Efficient third harmonic generation from metal–dielectric hybrid nanoantennas," Nano Lett. **17**, 2647–2651 (2017).
Sipe, J. E., So, V. C. Y., Fukui, M., and Stegeman, G. I., "Analysis of second-harmonic generation at metal surfaces," Phys. Rev. B **21**, 4389–4402 (1980).
Slenders, E., Bové, H., Urbain, M., Mugnier, Y., Sonay, A. Y., Pantazis, P., Bonacina, L., Vanden Berghe, P., vandeVen, M., and Ameloot, M., "Image correlation spectroscopy with second harmonic generating nanoparticles in suspension and in cells," J. Phys. Chem. Lett. **9**, 6112–6118 (2018).
Slenders, E., Hooyberghs, J., and Ameloot, M., "Coherent intensity fluctuation model for autocorrelation imaging spectroscopy with higher harmonic generating point scatterers—A comprehensive theoretical study," Phys. Chem. Chem. Phys. **17**, 18937–18943 (2015).
Smirnova, D. and Kivshar, Y. S., "Multipolar nonlinear nanophotonics," Optica **3**, 1241–1255 (2016).
Soavi, G. *et al.*, "Broadband, electrically tunable third-harmonic generation in graphene," Nat. Nanotechnol. **13**, 583 (2018).
Sordillo, L. A., Pu, Y., Pratavieira, S., Budansky, Y., and Alfano, R. R., "Deep optical imaging of tissue using the second and third near-infrared spectral windows," J. Biomed. Optics **19**, 056004 (2014).
Staedler, D. *et al.*, "Harmonic nanocrystals for biolabeling: A survey of optical properties and biocompatibility," ACS Nano **6**, 2542–2549 (2012).
Staedler, D. *et al.*, "Cellular uptake and biocompatibility of bismuth ferrite harmonic advanced nanoparticles," Nanomed.: Nanotechnol., Biol. Med. **11**, 815–824 (2015).
Stock, C., Zlatanov, K., and Halfmann, T., "Third harmonic generation and microscopy, enhanced by a bias harmonic field," Opt. Commun. **457**, 124660 (2020).
Sugiyama, N. *et al.*, "Effective labeling of primary somatic stem cells with $BaTiO_3$ nanocrystals for second harmonic generation imaging," Small **14**, 1703386 (2018).
Sun, X., Ji, Z., and He, S., "SHG-enhanced NIR-excited *in vitro* photodynamic therapy using composite nanoparticles of barium titanate and rose Bengal," RSC Adv. **9**, 8056–8064 (2019).
Tai, S. P., Wu, Y., Shieh, D. B., Chen, L. J., Lin, K. J., Yu, C. H., Chu, S. W., Chang, C. H., Shi, X. Y., Wen, Y. C., Lin, K. H., Liu, T. M., and Sun, C. K., "Molecular imaging of cancer cells using plasmon-resonant-enhanced third-harmonic-generation in silver nanoparticles," Adv. Mater. **19**, 4520–4523 (2007).
Terhune, R. W., Maker, P. D., and Savage, C. M., "Measurements of nonlinear light scattering," Phys. Rev. Lett. **14**, 681 (1965).
Thyagarajan, K., Rivier, S., Lovera, A., and Martin, O. J. F., "Enhanced second-harmonic generation from double resonant plasmonic antennae," Opt. Express **20**, 12860–12865 (2012).
Tilbury, K. and Campagnola, P. J., "Applications of second-harmonic generation imaging microscopy in ovarian and breast cancer," Perspect. Med. Chem. **7**, 21–32 (2015).
Timpu, F., Escalé, M. R., Timofeeva, M., Strkalj, N., Trassin, M., Fiebig, M., and Grange, R., "Enhanced nonlinear yield from barium titanate metasurface down to the near ultraviolet," Adv. Opt. Mater. **7**, 1900936 (2019a).
Timpu, F., Sendra, J., Renaut, C., Lang, L., Timofeeva, M., Buscaglia, M. T., Buscaglia, V., and Grange, R., "Lithium niobate nanocubes as linear and nonlinear ultraviolet Mie resonators," ACS Photonics **6**, 545–552 (2019b).
Valev, V. K., Silhanek, A. V., Verellen, N., Gillijns, W., Van Dorpe, P., Aktsipetrov, O. A., Vandenbosch, G. A. E., Moshchalkov, V. V., and Verbiest, T., "Asymmetric optical second-harmonic generation from chiral G-shaped gold nanostructures," Phys. Rev. Lett. **104**, 127401 (2010).
Van Steenbergen, V., Boesmans, W., Li, Z., de Coene, Y., Vints, K., Baatsen, P., Dewachter, I., Ameloot, M., Clays, K., and Berghe, P. V., "Molecular understanding of label-free second harmonic imaging of microtubules," Nat. Commun. **10**, 1–14 (2019).
Verma, M. S. and Chandra, M., "Nonlinear plasmonic sensing for label-free and selective detection of mercury at picomolar level," ACS Sens. **5**, 645–649 (2020).
Vuilleumier, J., Gaulier, G., De Matos, R., Ortiz, D., Menin, L., Campargue, G., Mas, C., Constant, S., Le Dantec, R., and Mugnier, Y., "Two-photon-triggered photorelease of caged compounds from multifunctional harmonic nanoparticles," ACS Appl. Mater. Interfaces **11**, 27443–27452 (2019).
Wang, J., Coillet, A., Demichel, O., Wang, Z., Rego, D., Bohuelier, A., Grelu, P., and Cluzel, B., "Saturable plasmonic metasurfaces for laser mode locking," Light Sci. Appl. **9**, 50 (2020).
Wang, K. *et al.*, "Quantum metasurface for multiphoton interference and state reconstruction," Science **361**, 1104–1108 (2018a).
Wang, T., Ouzounov, D. G., Wu, C., Horton, N. G., Zhang, B., Wu, C. H., Zhang, Y., Schnitzer, M. J., and Xu, C., "Three-photon imaging of mouse brain structure and function through the intact skull," Nat. Methods **15**, 789–792 (2018b).
Weber, N., Protte, M., Walter, F., Georgi, P., Zentgraf, T., and Meier, C., "Double resonant plasmonic nanoantennas for efficient second harmonic generation in zinc oxide," Phys. Rev. B **95**, 205307 (2017).
Weigelin, B., Bakker, G.-J., and Friedl, P., "Intravital third harmonic generation microscopy of collective melanoma cell invasion," Intravital **1**, 32–43 (2012).
Wolf, O., Campione, S., Benz, A., Ravikumar, A. P., Liu, S., Luk, T. S., Kadlec, E. A., Shaner, E. A., Klem, J. F., Sinclair, M. B., and Brener, I., "Phased-array sources based on nonlinear metamaterial nanocavities," Nat. Commun. **6**, 7667 (2015).
Yamashita, S., "Nonlinear optics in carbon nanotube, graphene, and related 2D materials," APL Photonics **4**, 034401 (2019).
Yariv, A., *Optical Electronics*, 4th ed. (Oxford University Press, 1995), ISBN: 978-0-19-510736-4.
Yazdanfar, S., Laiho, L. H., and So, P. T. C., "Interferometric second harmonic generation microscopy," Opt. Express **12**, 2739–2745 (2004).
Yoshikawa, N., Tamaya, T., and Tanaka, K., "High-harmonic generation in graphene enhanced by elliptically polarized light excitation," Science **356**, 736–738 (2017).
Yu, N., Genevet, P., Kats, M. A., Aieta, F., Tetienne, J.-P., Capasso, F., and Gaburro, Z., "Light propagation with phase discontinuities: Generalized laws of reflection and refraction," Science **334**, 333–337 (2011).
Yu, R., Cox, J. D., and Garcia de Abajo, F. J., "Nonlinear plasmonic sensing with nanographene," Phys. Rev. Lett. **117**, 123904 (2016).
Yu, Y. F., Zhu, A. Y., Paniagua-Domínguez, R., Fu, Y. H., Luk'yanchuk, B., and Kuznetsov, A. I., "High-transmission dielectric metasurface with 2π phase control at visible wavelengths," Laser Photonics Rev. **9**, 412–418 (2015).
Zavelani-Rossi, M., Celebrano, M., Biagioni, P., Polli, D., Finazzi, M., Cerullo, G., Duò, L., Labardi, M., Allegrini, M., Grand, J., and Adam, P.-M., "Near-field second-harmonic generation in single gold nanoparticles," Appl. Phys. Lett. **92**, 093119 (2008).
Zhang, Y., Grady, N. K., Ayala-Orozco, C., and Halas, N. J., "Three-dimensional nanostructures as highly efficient generators of second harmonic light," Nano Lett. **11**, 5519–5523 (2011).
Zhang, Y., Manjavacas, A., Hogan, N. J., Zhou, L., Ayala-Orozco, C., Dong, L., Day, J. K., Nordlander, P., and Halas, N. J., "Toward surface plasmon-enhanced optical parametric amplification (SPOPA) with engineered nanoparticles: A nanoscale tunable infrared source," Nano Lett. **16**, 3373–3378 (2016).
Zheng, G., Mühlenbernd, H., Kenney, M., Li, G., Zentgraf, T., and Zhang, S., "Metasurface holograms reaching 80% efficiency," Nat. Nanotechnol. **10**, 308–312 (2015).